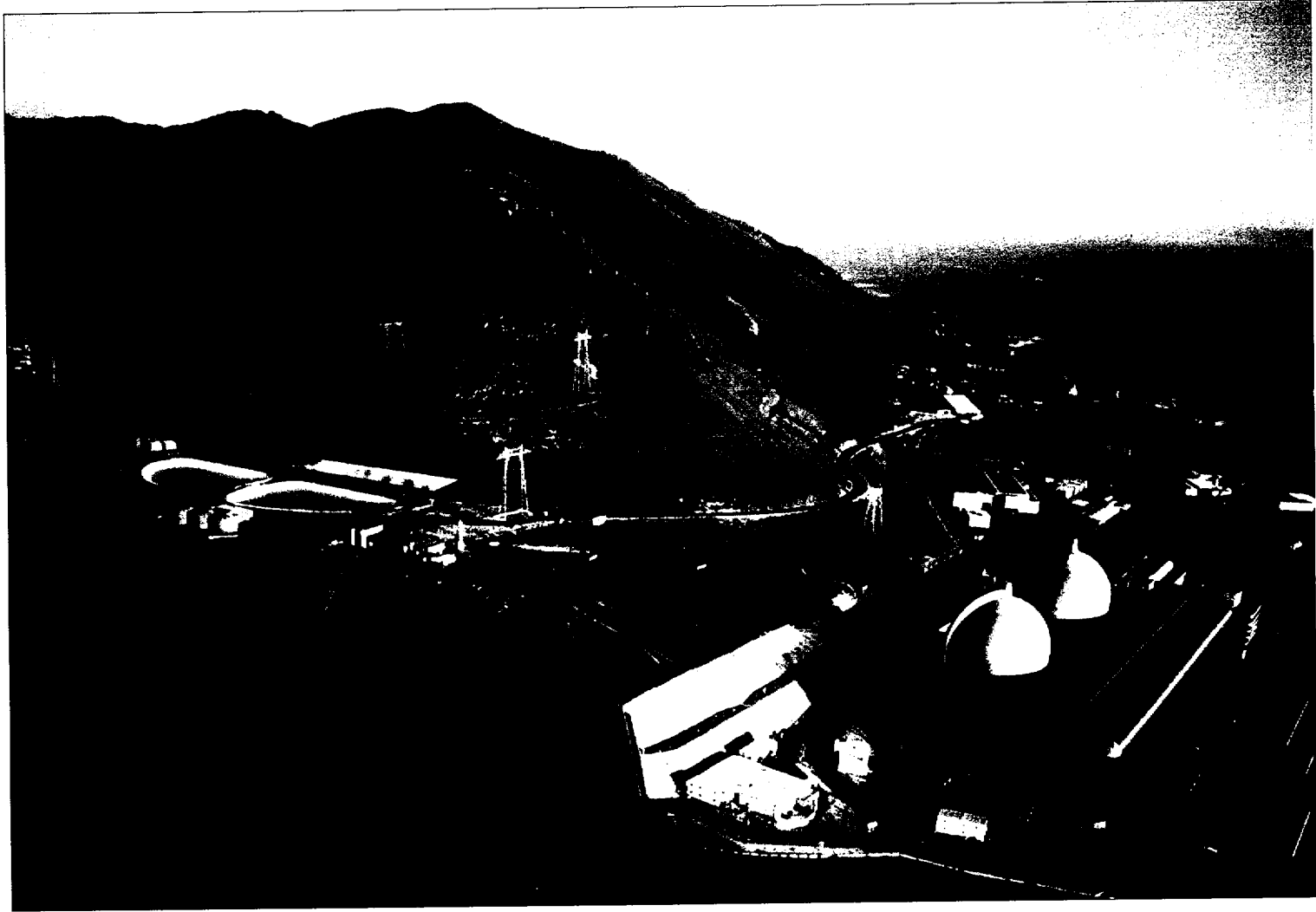


DIABLO CANYON

INDEPENDENT SPENT FUEL STORAGE INSTALLATION



CALCULATIONS



PACIFIC GAS AND ELECTRIC COMPANY

Title: Calculation Cover Sheet

PACIFIC GAS AND ELECTRIC COMPANY
GEOSCIENCES DEPARTMENT
CALCULATION DOCUMENT

Calc Number: GEO.DCPP.01.20

Revision: 1

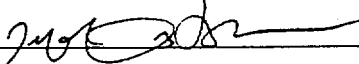
Date: November 6, 2001

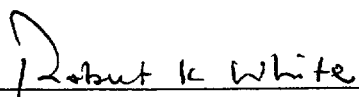
No. of Calc Pages: 61


Verification Method: A

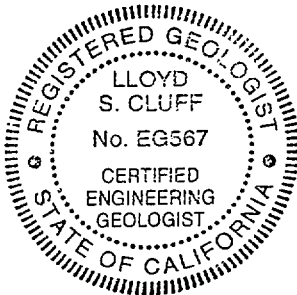
No. of Verification Pages: 1

TITLE Development of Strength Envelopes for Shallow Discontinuities at DCPP ISFSI using Barton Equations

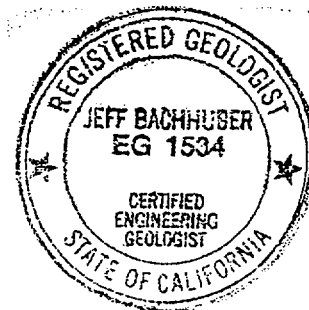
PREPARED BY  DATE November 6, 2001
Jeffrey L. Bachhuber William Lettis & Associates, Inc.
Printed Name Organization

VERIFIED BY  DATE 11/12/01
Robert K. White Geosciences
Printed Name Organization

APPROVED BY  DATE 11/13/01
Lloyd Cluff Geosciences
Printed Name Organization



Expires 12/31/02



DCPP ISFSI

CALCULATION PACKAGE GEO.DCPP.01.20

Development of Strength Envelopes for Shallow Discontinuities

at DCPP ISFSI Using Barton Equations

DCPP ISFSI
CALCULATION PACKAGE GEO.DCPP.01.20
Development of Strength Envelopes for Shallow Discontinuities
at DCPP ISFSI Using Barton Equations

Table of Contents

1.0	PURPOSE	6
2.0	INTRODUCTION	6
3.0	INPUTS	8
4.0	ASSUMPTIONS	9
5.0	METHOD	10
	5.1 Background	10
	5.2 Process	11
6.0	SOFTWARE	13
7.0	ANALYSIS	14
8.0	RESULTS	14
9.0	CONCLUSIONS	15
10.0	REFERENCES	16

List of Tables

Table 20-1. Barton Equation Input Parameters

List of Figures

- Figure 20-1. Joint roughness profiles (JRC) and typical range in roughness of joints, bedding planes, and faults.
- Figure 20-2. Dolomite Joint Shear Strength Curve A
- Figure 20-3. Dolomite Bedding Shear Strength Curve B
- Figure 20-4. Dolomite Faults Shear Strength Curve C
- Figure 20-5. Sandstone Joint Shear Strength Curve D
- Figure 20-6. Sandstone Bedding Shear Strength Curve E
- Figure 20-7. Sandstone Faults Shear Strength Curve F

List of Attachments

Attachment 1. Rock Engineering Course Notes, Chapter 4 (version dated Nov. 27, 2000),
E. Hoek, 2000

Table of Contents (continued)

List of Attachments (continued)

Attachment 2. Barton Spreadsheet Verification Runs

Attachment 3. ISFSI Site Barton Shear Strength Calculation Runs

DCPP ISFSI GEOTECHNICAL CALCULATION PACKAGE

Title: Development of strength envelopes for shallow discontinuities at DCP
ISFSI using Barton equations

Calc Number: GEO.DCPP.01.20

Revision: Rev. 01

Author: Jeff L. Bachhuber

Date: September 21, 2001

Verifier: Robert K. White

1.0 PURPOSE

The purpose of this calculation package is to use the Barton equation to estimate the shear strength for in situ rock discontinuities (joints, bedding planes, and faults) in the relatively hard, non-friable dolomite and sandstone bedrock at the ISFSI and CTF sites, and within the slope above the ISFSI pads (Barton and Choubey, 1977; Hoek and others, 1995; Hoek, 2000).

2.0 INTRODUCTION

The Barton equation estimates the in situ shear strength of naturally occurring rock discontinuities in relatively hard rock on the basis of field and laboratory measurements of discontinuity properties. Shear strength envelopes developed in this calculation package for discontinuity surfaces within the shallow rock mass at the DCP ISFSI site are used in the stability analyses of surficial rock mass sliding, wedge, and topple slope failures in the proposed cutslope above the ISFSI (Calculation Package GEO.DCPP.01.23), and frictional sliding along shallow rock discontinuities below the foundation of the ISFSI pads (Calculation Package GEO.DCPP.01.04).

Unconfined, stress-relieved rock in the near surface and in future excavation cuts are free to dilate along pre-existing discontinuities. The Barton equation models in situ discontinuity shear strength within this zone. The stress-relieved zone is known from borings and trenches (William Lettis and Associates, Inc. (2001) Diablo Canyon ISFSI Data Report B and D) to be about 4 feet deep, and is conservatively estimated to extend

20 feet below the existing ground surface, and extend for about 20 feet behind the proposed ISFSI cutslopes. Deeper rock below the surficial stress-relieved zone is tightly confined and interlocked, limiting shear plane development along continuous joints and block dilation or rotation. Deep-seated or large-scale rock slope failures in the ISFSI site area require interconnection of numerous individual discontinuities and breakage of large asperities, rock bridges, and unjointed rock. The Barton equation is not appropriate to model the rock mass strength for the tightly confined rock and evaluation of potential deep-seated failures. For these conditions, the Hoek-Brown criterion (Hoek, 2000; Calculation Package GEO.DCPP.01.19) was instead used for estimation of the in situ rock mass shear strength. Similarly, the Barton equation is not appropriate to model the shear strength for continuous clay beds that have been found within the dolomite and sandstone. Clay bed shear strength is estimated on the basis of direct shear testing of clay samples as described in Calculation Package GEO.DCPP.01.31. The Barton equation also is not applicable for the softer, friable dolomite (Unit Tof_{b-1a}) and sandstone (Unit Tof_{b-2a}) that appear to be controlled by cementation and grain-grain frictional strength rather than by discontinuity strength (Calculation Packages GEO.DCPP.01.21 and 01.16).

Sliding resistance, or shear strength, along a natural rock discontinuity is controlled both by the inherent frictional characteristics of the rock, and by interlocking of natural undulations and irregularities (asperities) on the surface (Hoek and others, 1995; Hoek, 2000). The strength contribution imparted by the surface roughness of the discontinuity is dependant on the magnitude of normal stress. At low normal stresses, shear displacement along joint surfaces involves dilation of the joint as asperities on the surfaces override one another (Barton and Choubey, 1977). At high levels of normal stress, the rock mass is no longer free to dilate, and asperity interlocking on the discontinuity surface resists sliding until shearing stress is sufficient to break off asperities, bringing the strength of the rock into play. Therefore, the strength of the rock discontinuity typically increases with increasing confining stress, and significant "apparent cohesion" (y-axis intercept) is developed with depth as a result of strength contribution from asperities. The Barton equation was developed on the basis of laboratory testing of natural rock specimens (e.g., Barton, 1976; Barton and Choubey, 1977; Barton and Bandis, 1990), and factors the interrelationship between discontinuity surface roughness, normal stress, and shear strength. The Barton equation is described in an online website document entitled "Rock Engineering Course Notes" (Hoek, 2000). Excerpts from Chapter 4 of the course notes, "Shear strength of discontinuities," explain the Barton equation and are included in

Attachment 1 of this calculation package. The Barton shear strength equation is as follows:

$$\tau = \sigma_n \tan(\text{JRC} \log_{10} (\text{JCS}/\sigma_n) + \phi_b)$$

τ = shear strength

JRC = joint roughness coefficient

JCS = joint compressive strength

σ_n = effective normal stress

ϕ_b = base friction angle

The Barton equation develops non-linear shear strength envelopes for rock mass discontinuities.

For the ISFSI site, the Barton equation was used to evaluate strength separately for the dolomite and sandstone bedrock, and for three types of discontinuities that could exhibit different behavior: bedding planes, joints, and faults. Differences in mineralogy and cementation influence the strength of dolomite and sandstone. Differences in the joint surface roughness (e.g., JRC), wall alteration, clay infilling, and texture between bedding planes, joints, and faults result in variations of strength. Therefore, separate shear strength curves were developed for each rock and discontinuity type to evaluate strength differences and capture the range of strength at the ISFSI site.

3.0 INPUTS

The Barton equation uses three input parameters to estimate rock mass strength: (1) the basic (“base” herein) friction angle of sawcut or lightly ground rock surfaces; (2) the Joint Roughness Coefficient (JRC); and, (3) the Joint Compressive Strength (JCS). Table 20-1 shows the values used for the Barton equation. These values are derived from statistical analyses of data from William Lettis & Associates, Inc. (2001) Diablo Canyon ISFSI Data Report F (JRC), and Calculation Packages GEO.DCPP.01.17 (JCS) and GEO.DCPP.01.18 (base friction angle).

The Barton equation models shear strength along rock discontinuities in the ISFSI site area for failure modes that involve sliding along one or several, distinct, continuous joints and bedding. The basic data are provided in William Lettis & Associates, Inc. (2001) Diablo Canyon ISFSI Data Reports B, D, and F.

4.0 ASSUMPTIONS

The following assumptions were used for development of shear strength envelopes for discontinuities at the ISFSI site.

1. The shear strength of the rock mass is dependant on the confining pressure, and the non-linear failure envelope predicted by the Barton equation is assumed to closely approximate the conditions at the DCPD ISFSI site. This assumption is generally reasonable as presented in Hoek (2000). Excerpts of relevant pages from Hoek (2000) are included in Attachment 1.
2. In situ characterization of the joint roughness coefficient (JRC) for discontinuities represents both the range of, and typical properties at, the DCPD ISFSI site. This assumption is reasonable because a large data set of field observations is used, as presented in William Lettis & Associates, Inc. (2001) Diablo Canyon ISFSI Data Report F.
3. Laboratory direct shear tests of rock core discontinuities from ISFSI site exploratory borings represent the range of base friction angles for in situ discontinuity surfaces in dolomite and sandstone. This assumption is reasonable as presented in Calculation Package GEO.DCPP.01.18.
4. The joint compression strength (JCS) of discontinuities is equivalent to 25% of the laboratory-determined uniaxial compressive strength of rock core obtained from the ISFSI and CTF site boreholes. This assumption is conservative, as presented in Franklin and Dussealt (1989) and discussed below. The uniaxial (unconfined) compression test data is presented in Calculation Package GEO.DCPP.01.17.

5.0 METHOD

5.1 Background

The base friction angle is the inherent frictional property between two relatively smooth rock surfaces, and is dependent on mineralogy, grain size, and texture (Barton and Bandis, 1990; Hoek, 2000). The base friction angle is estimated by comparison of rock types with literature-reported values, or by making laboratory direct shear or sliding measurements on saw-cut or lightly ground rock surfaces. We estimated base friction angles for the dolomite and sandstone at the ISFSI site on the basis of laboratory direct shear testing of joints, bedding planes, and faults in core samples from exploratory borings as described in Calculation Package GEO.DCPP.01.18. Table 20-1 lists the range in base friction angles for dolomite and sandstone in the ISFSI site area. As discussed in Calculation Package GEO.DCPP.01.18, direct shear test data were parceled into three groups to develop estimated failure envelope curves on the basis of the condition of the discontinuity surface: clean rock-rock discontinuities; clay-coated discontinuities; and, a combination of clean rock and clay-coated discontinuities. These three conditions represent the range in shear strength for clean joints and bedding parting surfaces (rock-rock contacts), and clay-coated joints, bedding, or fault planes (clay-clay and/or rock-clay contacts). The post-peak failure envelopes from each group of discontinuity types were then used to determine average friction angles for each condition. The derived friction angles for the clean rock-rock and clay-coated test data are used to represent the upper and lower bound base friction angles for the rock discontinuities, respectively. The post-peak friction angle determined from the failure envelope for the combined rock-rock and clay-coated data is used to represent the average base friction angle for rock mass discontinuities (Table 20-1).

Joint Roughness Coefficient (JRC) is a quantification of discontinuity surface roughness to account for the strength influence of the incident angle of asperity surfaces (William Lettis & Associates, Inc. (2001) Diablo Canyon ISFSI Data Report F). These values are determined in the field or laboratory either by direct measurement, or by comparison with

standardized roughness profiles (Barton and Choubey, 1977) (Figure 20-1). The JRC values are estimated for hundreds of discontinuity surfaces exposed in ISFSI site exploratory trenches using the roughness profile comparison. The field-determined JRC values were compiled and statistically evaluated (using an Excel spreadsheet) to determine the mean values and standard deviation for the data set (presented in Tables F-1 and F-2 in William Lettis & Associates, Inc. (2001) Diablo Canyon ISFSI Data Report F). Table 20-1 presents mean JRC values, standard deviation, and mean plus and minus one standard deviation values for JRC that were used in the Barton equation.

The Joint Compressive Strength (JCS) represents the strength required to break asperities, and corresponds to the compressive strength of rock on the discontinuity surface. The JCS accounts for weathering-induced strength degradation of the rock block surfaces. JCS typically is obtained by Schmidt hammer rebound testing of rock surfaces, or by applying a reduction factor to the unconfined compressive strength of intact rock blocks (Barton and Bandis, 1990; Hoek, 2000, Franklin and Dusseault, 1989). Franklin and Dusseault (1989) report that using one-quarter of the uniaxial compressive strength of intact rock core gives a realistic approximation of lower-bound shear strength for discontinuities with thin altered layers. We conservatively assumed JCS values that are 25% of the laboratory-determined unconfined strength of rock cores from the exploratory borings as described in Calculation Package GEO.DCPP.01.17.

5.2 Process

The Barton analyses was performed in a step-by-step process, as described below. Input data described above were used in Excel spreadsheets created by Jeff Bachhuber of William Lettis & Associates, Inc.

Step 1

Excel spreadsheet functions were used to calculate the mean and one-sigma standard deviation JRC values separately for dolomite and sandstone, and for the three types of discontinuities: joints, bedding planes, and faults. The mean and standard deviation range of values of JRC were used for input into the Barton equation.

Step 2

An Excel spreadsheet was developed based on formulas provided in an example spreadsheet presented in Hoek (2000). The example spreadsheet was used to verify the Excel spreadsheet. Input parameters from the example problem were input into the spreadsheet, and the output was compared against the example problem. The spreadsheet successfully emulated the example problem. A copy of the example problem and spreadsheet verification output file are included in Attachment 2.

Step 3

Input data was entered into the verified Barton Excel spreadsheet, and individual workbooks were established for dolomite and sandstone analyses. Separate spreadsheets were prepared within each workbook to evaluate the shear strength of joints, bedding planes, and fault planes. The mean and standard deviation spread of values were entered for JRC and JCS data. The range in laboratory test-determined post-peak friction angles for rock-rock, and clay-coated discontinuities was used to bound the upper and lower bound values for base friction angle. The friction angle estimated from the combined rock-rock and clay-coated direct shear post-peak failure envelope was used as a mean value for the rock mass. Output files were checked and compared against each other to evaluate the sensitivity of strength to variation of input parameters.

Step 4

The Barton spreadsheet output files were used to develop a series of stress-strain failure envelopes for the rock discontinuities. Each failure envelope was plotted in the program SPSS DeltaGraph to obtain exact 1:1 vertical and horizontal scales for accurate plotting of the failure envelopes and evaluation of angle of internal friction (ϕ angle) and cohesion intercept (c). The following six failure envelopes were developed:

- Dolomite Joint Shear Strength - Figure 20-2
- Dolomite Bedding Plane Shear Strength - Figure 20-3
- Dolomite Fault Plane Shear Strength - Figure 20-4
- Sandstone Joint Shear Strength - Figure 20-5
- Sandstone Bedding Plane Shear Strength - Figure 20-6
- Sandstone Fault Plane Shear Strength - Figure 20-7

6.0 SOFTWARE

Statistical analyses and derivation of the Barton shear strength failure envelopes were performed using Microsoft Excel software on a DELL Inspiron model 8000 laptop computer. Final DeltaGraph curves were prepared on an Apple Macintosh G3 computer. The software specifications are as follows:

Apple Operating System - Version 8.5.1, 1998

Microsoft Windows ME - Version 4.90.3000, 2000

Microsoft Excel - Version 9.03821 SR-1, 2000

SPSS DeltaGraph - Version 4.0.5C, 1997

Data tabulation and statistical analyses were performed using standard Excel functions. The Barton equation calculations were performed using an Excel spreadsheet created by Jeff Bachhuber, using equations presented in Hoek (2000). The spreadsheet cell equations are shown on Chapter 4, page 71 of "Rock Engineering Course Notes" (revision date of December, 2000). The spreadsheet was verified as described in Step 2 above, using method 1 of GEO.001 Section 4.2.2, and the following was identified:

- a) Spreadsheet name: btndolojoints.Rev3, btndolobddg+faults.Rev3; btNSSbddg+faults.Rev2; and, btNSSjointsfinal.Rev2.
- b) Spreadsheet version: (not applicable)
- c) Spreadsheet revision: Rev1 dated 7/12/2001.
- d) Computer platform compatibility: Windows ME
- e) Spreadsheet capabilities and limitations: The spreadsheet generates shear strength failure envelopes using the Barton equation (Hoek, 2000). The spreadsheet is a modified version of the spreadsheet described in Attachment 1. Strength envelopes are valid when ranges of input variables are within those described in Attachment 1.
- f) Spreadsheet test cases: described in Attachment 2.
- g) Instructions for use: input values for variables base friction angle, JRC, and JCS as described in Attachment 1.
- h) Spreadsheet author: Jeff Bachhuber.

- i) Identification of individual responsible for controlling the software or executables: see Geosciences QA procedures CF2.GEI.
- j) Change control: see Geosciences QA procedures CF2.GEI.
- k) Verification methods used: method 1 as shown in Attachment 2.

7.0 ANALYSIS

Multiple analyses were performed to evaluate the differences in shear strength between discontinuities in dolomite and sandstone, and to assess the sensitivity of shear strength to variations in the three input parameters (base friction angle, JRC, JCS). Spreadsheet output files are included in Attachment 3, and calculated shear strength failure envelopes are presented in Figures 20-2 through 20-7. The output files and failure envelopes were visually compared with each other to verify correct plotting of data. The plots were also visually compared with each other to evaluate the sensitivity of discontinuity strength to changes in input parameters, and to evaluate the strength differences between dolomite and sandstone, and joints, bedding planes, and fault planes.

8.0 RESULTS

Attachment 3 presents the Barton Excel spreadsheet output files. The calculated shear strength envelopes developed by the Barton spreadsheet were replotted with the DeltaGraph program for presentation of results. The final failure envelope plots are presented in Figures 20-2 through 20-7.

All failure envelopes exhibit typical non-linear shapes that are characteristic of natural rock joints (Hoek and others, 1995; Hoek, 2000). The estimated rock mass discontinuity shear strengths are higher than the laboratory test base friction angle, and show the strength influence of normal stress (confining stress) variation, asperity roughness (JRC), and uniaxial compressive strengths of discontinuity wall rock (JCS).

Comparison of shear strength envelopes shows that the mean and upper bound joint shear strengths for dolomite are about 105% to 130% higher than that for the sandstone. The strength differences are primarily the result of higher base friction angle and JCS for the dolomite, as the range in JRC values are relatively similar. For dolomite, the lower and

upper bound and mean shear strengths for joint and fault surfaces are similar. The lower and mean value shear strengths for dolomite bedding planes are similar to those for the dolomite joints and faults, but the upper bound strength for bedding planes is lower (Figures 20-2, 20-3, 20-4). The shear strengths for sandstone joints, faults, and bedding planes are similar for lower and upper bound and mean values (Figures 20-5, 20-6, and 20-7).

For analyses of shallow rock slide and wedge failures, or shallow foundation sliding along discrete rock discontinuities, the portions of the failure envelopes between 0 and about 0.15 MPa normal stress range are appropriate. Straight tangent line approximations of the friction angle values at the midpoint of this stress range are also plotted in Figures 20-2 through 20-7. Calculated in situ friction angles for these portions of the curves range between about 17.5° and 54° for dolomite, and 16° to 46° for sandstone. These values are somewhat higher than the base friction angles of between 14° and 38° for dolomite, and 14° and 32° for sandstone. Mean shear strength values range between 33° and 36° for dolomite, and 26.5° and 31° for sandstone. These values are within the range of typical friction angles for discontinuities in similar rock types reported in the literature (e.g., Franklin and Dussealt, 1989).

9.0 CONCLUSIONS

The discontinuity shear strength failure envelopes for ISFSI site dolomite and sandstone calculated using the Barton equation, and the straight-line fits to the envelopes in the low-stress range, are suitable for estimating the in situ rock mass strength for the following uses: (1) slope stability analyses of shallow rock slide and wedge failures at proposed ISFSI cutslopes; and, (2) foundation sliding resistance along shallow joint, fault, and bedding surfaces. Analyses should consider the entire range in strength (mean, upper and lower bound) shown by the failure envelope curves, and differences between sandstone and dolomite. For most cases, it is reasonable to use the calculated mean curves as the best representation of in situ rock mass strength, which range between 33° and 36° for dolomite, and 26.5° and 31° for sandstone. The lower-bound strength curves should be considered when persistent low-strength discontinuities are being modeled, such as gouge-filled fault planes.

10.0 REFERENCES

- Barton, N.R., 1976, The shear strength of rock and rock joints: International Hour. Mech. Min. Science & Geomechanics Abstract, Vol. 13 (10), pp. 1-24.
- Barton, N.R., and Bandis, S.C., 1990, Review of predictive capabilities of JRC-JCS model in engineering practice: in Barton, N.R. and Stephansson, O., editors, Rock joints, Proceedings international symposium on rock joints: Loen, Norway: published by Balkema, Rotterdam, pp. 603-610.
- Barton, N.R. and Choubey, V., 1977, The shear strength of rock joints in theory and practise: Rock Mechanics, Vol. 10 (1-2), pp. 1-54.
- Franklin, J.A., and Dussealt, M.B., 1989, Rock Engineering, McGraw Hill, page 67.
- Hoek, E., 2000, Rock engineering course notes: on-line document www.roscience.com/roc/Hoek/Hoeknotes, version dated December [November in Attachment 1], 2000.
- Hoek, E., Kaiser, P.K., and Bawden, W.F., 1995, Support of underground excavations in hard rock: A.A. Balkema, Rotterdam, pp. 48 to 56.
- Microsoft Excel '98, Microsoft Corporation, Redmond, WA.
- SPSS Delta Graph, 1997.
- William Lettis & Associates, Inc., 2001, Letter to Robert White, PG&E Geosciences from Robert C. Witter, November 5, 2001, Completion of Data Reports transmitting Data Reports A through K to PG&E Geosciences Department;
- Diablo Canyon ISFSI Data Report B - Borings in ISFSI Site Area, Rev. 0, November 5, 2001, prepared by J. Bachhuber, 244 p.
- Diablo Canyon ISFSI Data Report D - Trenches in the ISFSI Site Area, Rev. 0, November 5, 2001, prepared by J. Bachhuber, 66 p.
- Diablo Canyon ISFSI Data Report F - Field Discontinuity Measurements, Rev. 0, November 5, 2001, prepared by C. Brankman and J. Bachhuber, 85 p.
- Diablo Canyon ISFSI Data Report H - Rock Strength Data and GSI Sheets, Rev. 0, November 5, 2001, prepared by J. Bachhuber, 37 p.
- Diablo Canyon ISFSI Data Report I - Rock Laboratory Test Data (GeoTest Unlimited), Rev. 0, November 5, 2001, prepared by J. Sun, 203 p.

Geosciences Calculation packages

GEO.DCPP.01.04	Methodology for determining sliding resistance along base and sides of DCPP ISFSI pad
GEO.DCPP.01.16	Development of strength envelopes for non-jointed rock at DCPP ISFSI based on laboratory data
GEO.DCPP.01.17	Determination of mean and standard deviation unconfined compression strengths for hard rock at DCPP ISFSI based on laboratory tests
GEO.DCPP.01.18	Determination of basal friction angle along rock discontinuities at DCPP ISFSI based on laboratory tests.
GEO.DCPP.01.19	Development of strength envelopes for jointed rock mass at DCPP ISFSI using Hoek-Brown equations
GEO.DCPP.01.20	Development of strength envelopes for shallow discontinuities at DCPP ISFSI using Barton equations
GEO.DCPP.01.21	Analysis of bedrock stratigraphy and geologic structure at the DCPP ISFSI site
GEO.DCPP.01.23	Pseudostatic wedge analysis of DCPP ISFSI cutslope (SWEDGE analysis)
GEO.DCPP.01.31	Development of strength envelopes for clay beds

QA Documentation

PG&E Quality Assurance Procedure GEO.001, Development and Independent Verification of Calculations for Nuclear Facilities

PG&E Quality Assurance Procedure CF2.GE1, Verification and Change Control of Quality-related Software

WLA "Work Plan and Technical Procedure for Geologic Mapping" dated April, 1998, and revised in April, 2001.

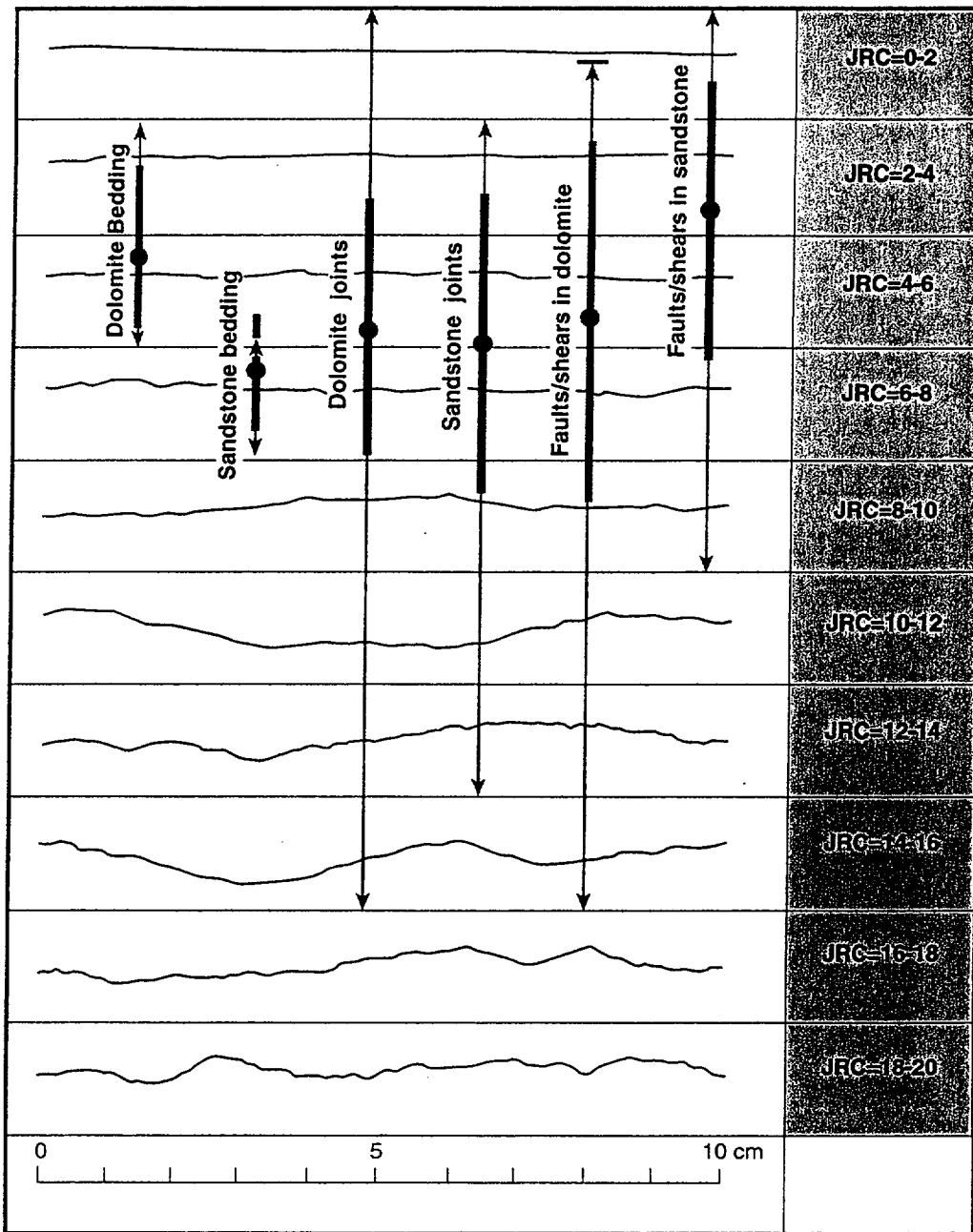
Table 20-1. Barton Equation Input Parameters

DOLOMITE		Base friction Angle (ϕ_b) ¹	Joint Roughness Coefficient ² (JRC)		Joint Compressive Strength ³ (JCS)
Joint	range	14-38	range	0-16	
			std. dev.	2.3	
	combined rock-rock & clay-coated	26.0 (ave.)	mean	5.6	8.0
	rock-rock	38.0	mean + s.d.	7.9	11.8
	clay-coated	14.0	mean - s.d.	3.3	4.3
Bedding	range	14-38	range	2-6	
			std. dev.	1.2	
	combined rock-rock & clay-coated	26.0 (ave.)	mean	4.4	8.0
	rock-rock	38.0	mean + s.d.	5.6	11.8
	clay-coated	14.0	mean - s.d.	3.2	4.3
Faults/Shears	range	14-38	range	1-16	
			std. dev.	3.2	
	combined rock-rock & clay-coated	26.0 (ave.)	mean	5.5	8.0
	rock-rock	38.0	mean + s.d.	8.7	11.8
	clay-coated	14.0	mean - s.d.	2.3	4.3
SANDSTONE		Base friction Angle (ϕ_b) ¹	Joint Roughness Coefficient ² (JRC)		Joint Compressive Strength ³ (JCS)
Joint	range	14-32	range	2-14	
			std. dev.	2.64	
	combined rock-rock & clay-coated	21 (ave.)	mean	6.0	5.5
	rock-rock	32	mean + s.d.	8.6	7.75
	clay-coated	14	mean - s.d.	3.4	3.25
Bedding	range	14-32	range	6-8	
			std. dev.	1	
	combined rock-rock & clay-coated	21 (ave.)	mean	6.5	5.5
	rock-rock	32	mean + s.d.	7.5	7.75
	clay-coated	14	mean - s.d.	5.5	3.25
Faults/Shears	range	14-32	range	0-10	
			std. dev.	2.27	
	combined rock-rock & clay-coated	21 (ave.)	mean	3.6	5.5
	rock-rock	32	mean + s.d.	5.9	7.75
	clay-coated	14	mean - s.d.	1.3	3.25

Notes: ¹ Base friction angle measured from direct shear testing of rock core from ISFSI site borings, as described in DCPD ISFSI SAR Section 2.6 Topical Report Appendix I, and Calculation Package GEO.DCPP.01.18.

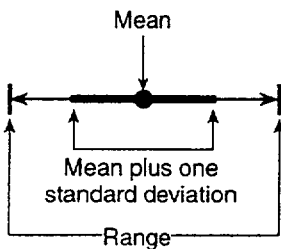
² Joint Roughness Coefficient (JRC; Barton, 1977) compiled from field measurements of discontinuity roughness using the Barton standard JRC profiles (Barton and Bandis, 1990), and presented in Tables F-1 and F-2 in DCPD ISFSI SAR Section 2.6 Topical Report Appendix F.

³ Joint Compressive Strength (JCS) is taken as 25% of intact rock core unconfined compressive strength presented in DCPD ISFSI SAR Section 2.6 Topical Report Appendix I, and Calculation Package GEO.DCPP.01.17. This approach conservatively estimates the strength of discontinuity surfaces with thin altered coatings (Franklin and Dusseault, 1989).



Note: JRC = Joint roughness coefficient

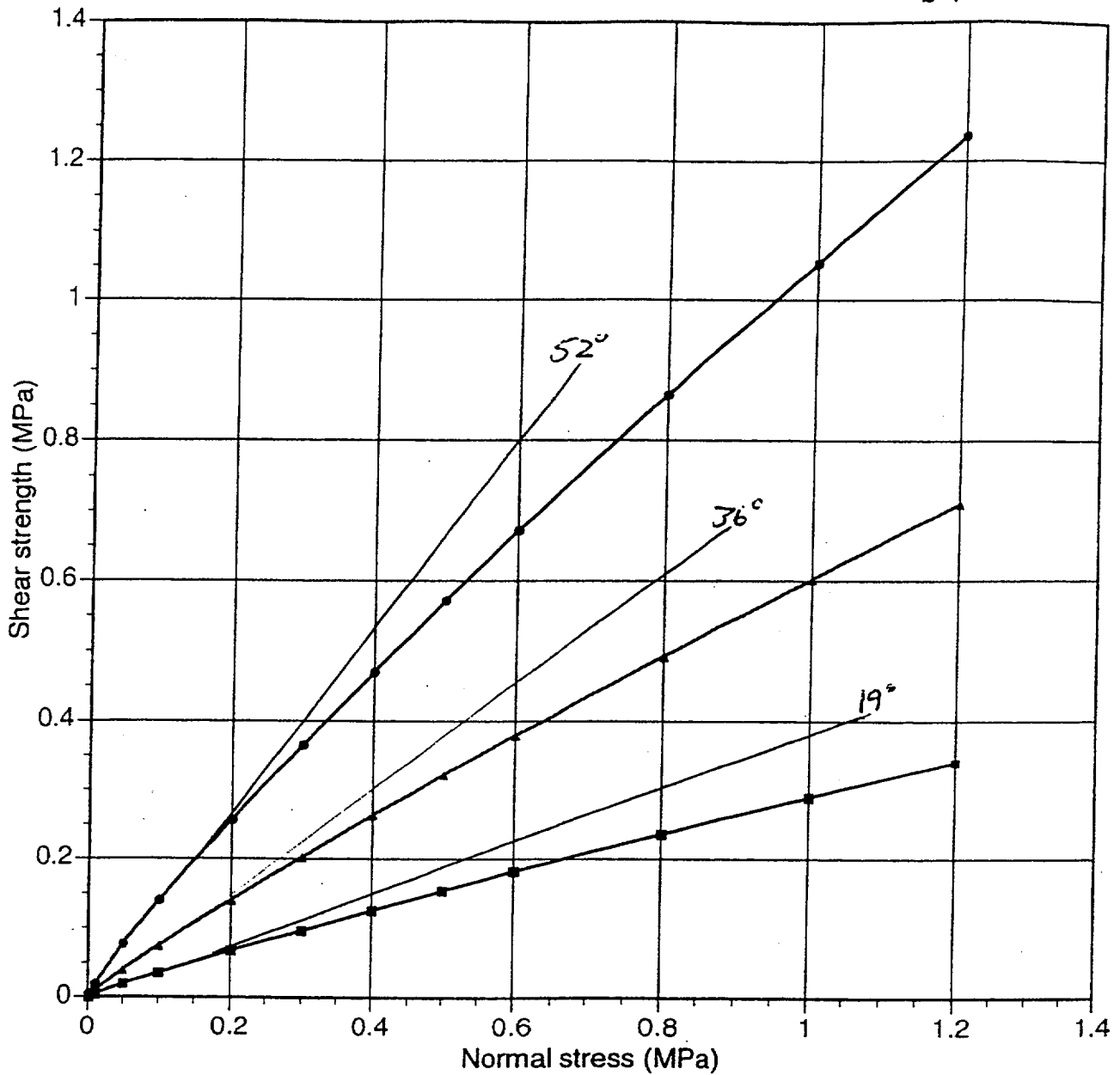
Chart from Barton and Choubey (1977)



Range in roughness for fractures in dolomite (Unit Tof_{b-1}) and sandstone (Unit Tof_{b-2}) in ISFSI site area.

Figure 20-1. Joint roughness profiles (JRC) and typical range in roughness of joints, bedding planes, and faults.

Comparison of Barton joint strength ranges - Dolomite (Tof_{b-1})



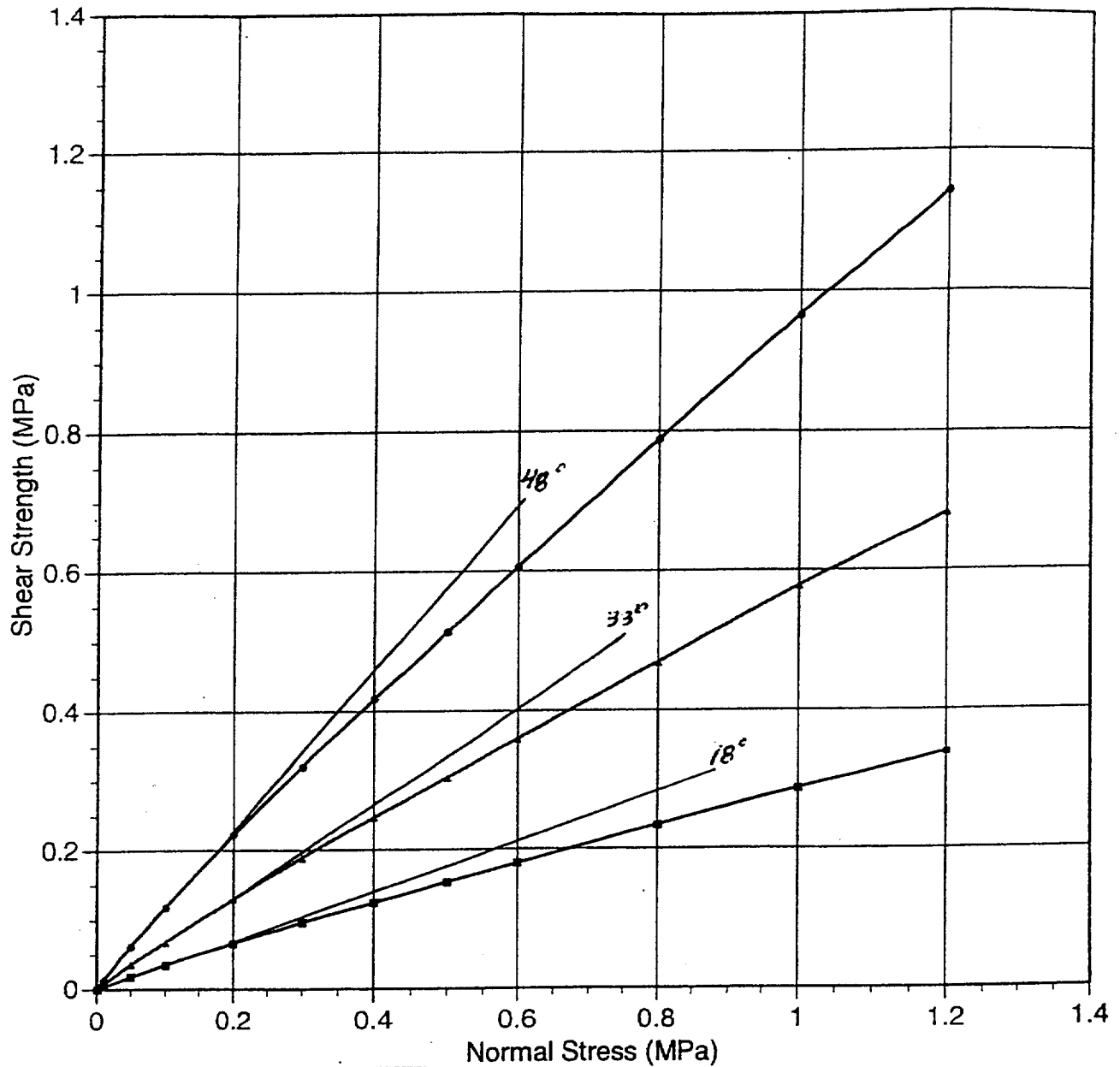
—●— Lower bound
 —▲— Upper bound
 —◆— Mean

Note: Upper and lower bounds for JRC and JCS represent one standard deviation above and below the mean values, respectively. Upper and lower bounds for basal friction angle are based on a range of strength envelopes for clean joints (upper bound), clay-coated joints (lower bound), and combination of both (mean). Curves compiled from Attachment 3, pages 44 - 46.

36° Tangent line drawn tangent to the curve at the midpoint of normal stress range (0 to 0.15 MPa).

Figure 20-2. Dolomite Joint Shear Strength Curve A

Comparison of Barton bedding strength ranges - Dolomite (T_{b-1})



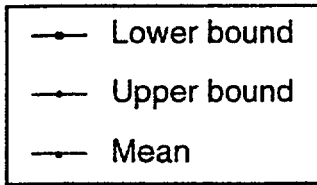
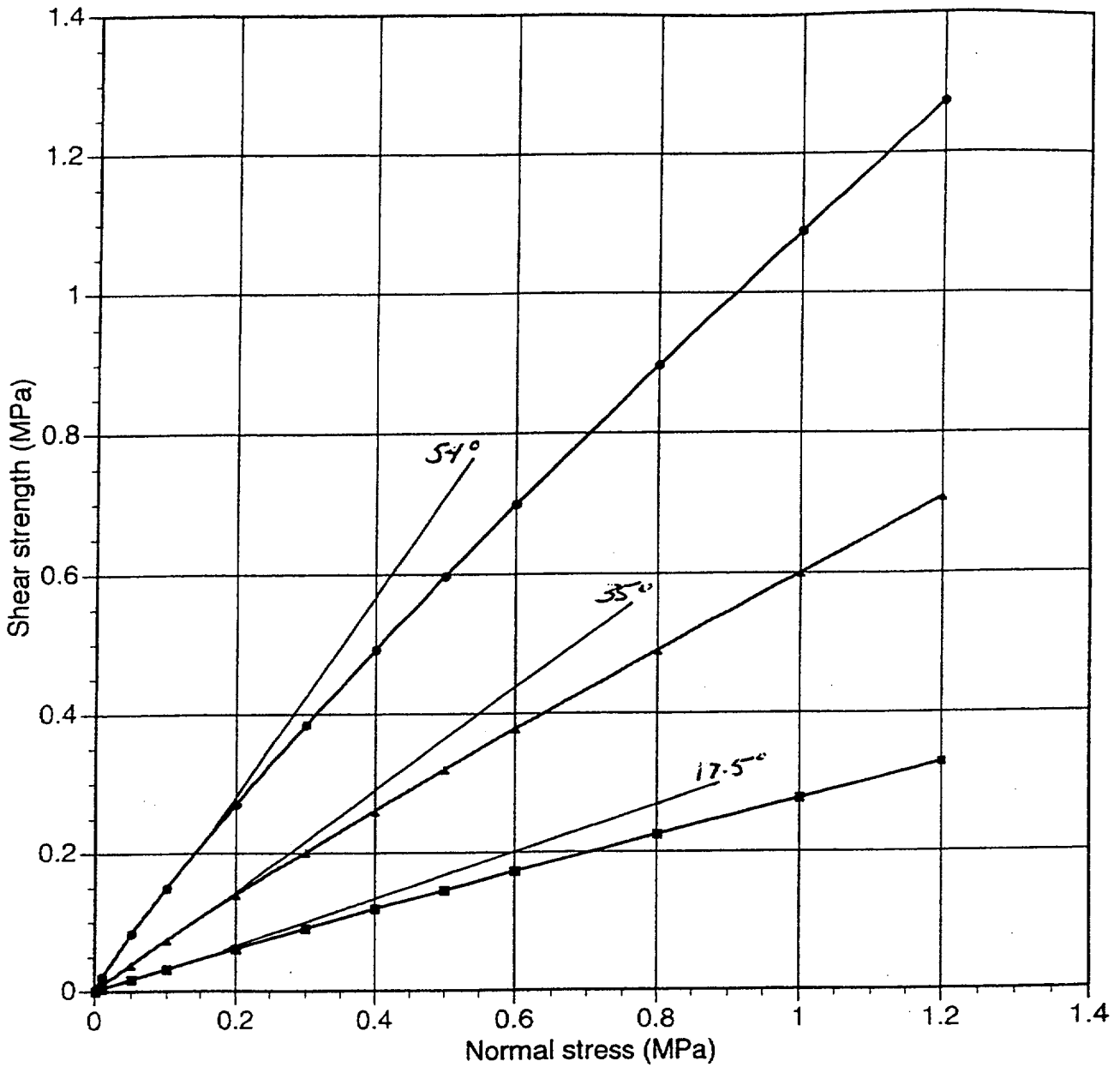
—●— Lower bound
 —●— Upper bound
 —●— Mean

36° Tangent line drawn
 tangent to the curve at the
 midpoint of normal stress
 range (0 to 0.15 MPa).

Note: Upper and lower bounds for JRC and JCS represent
 one standard deviation above and below the mean values,
 respectively. Upper and lower bounds for basal friction
 angle are based on a range of strength envelopes for
 clean joints (upper bound), clay-coated joints (lower
 bound), and combination of both (mean). Curves
 compiled from attachment 3, pages 47 - 49.

Figure 20-3. Dolomite Bedding Shear Strength Curve B

Comparison of Barton fault strength ranges - Dolomite (Tof_{b-1})

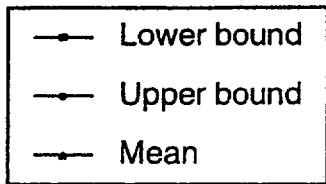
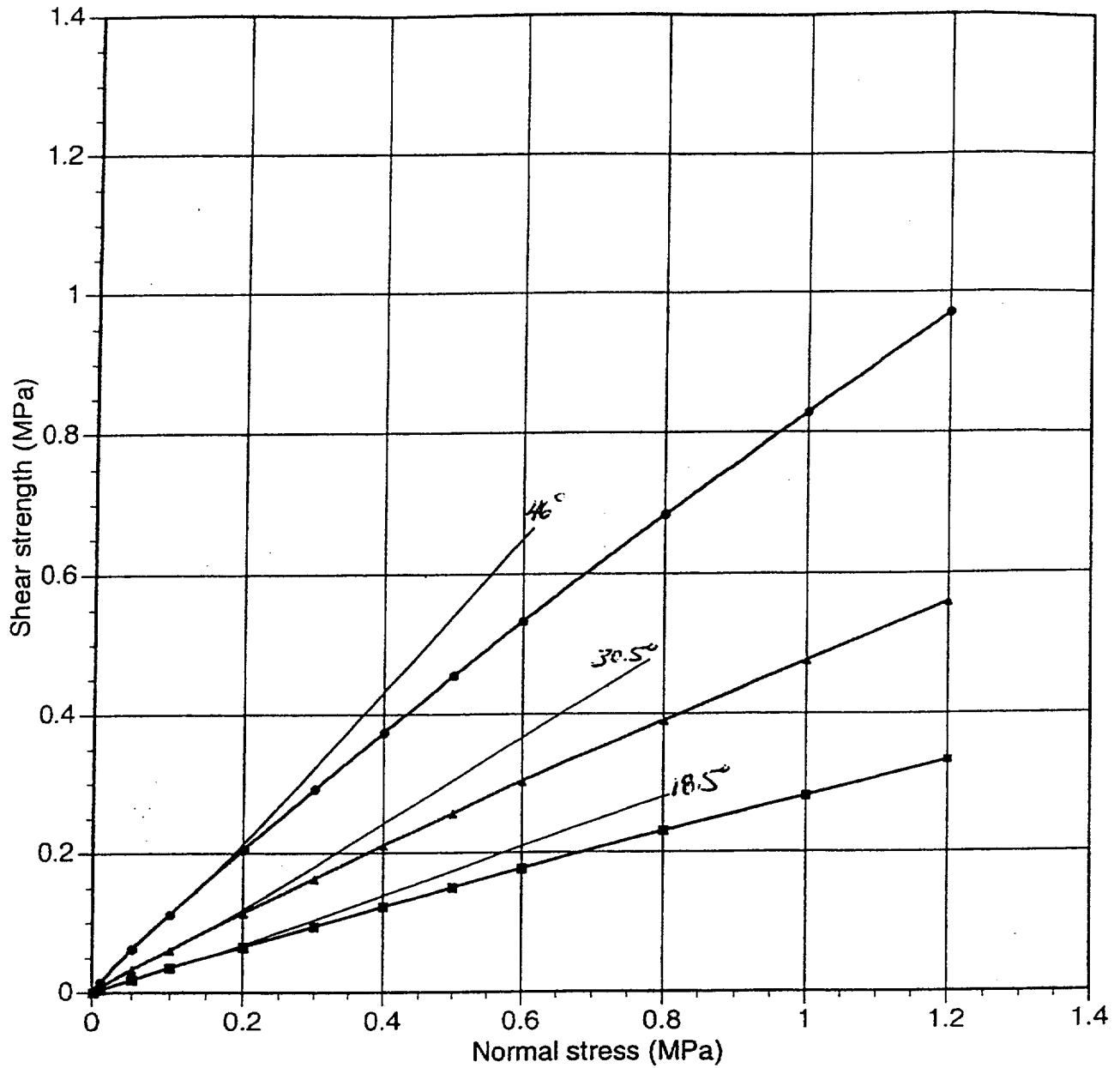


Note: Upper and lower bounds for JRC and JCS represent one standard deviation above and below the mean values, respectively. Upper and lower bounds for basal friction angle are based on a range of strength envelopes for clean joints (upper bound), clay-coated joints (lower bound), and combination of both (mean). Curves compiled from Attachment 3, pages 50 - 52.

36° Tangent line drawn tangent to the curve at the midpoint of normal stress range (0 to 0.15 MPa).

Figure 20-4. Dolomite Faults Shear Strength Curve C

Comparison of Barton joint strength ranges - Sandstone (Tof_{b-2})

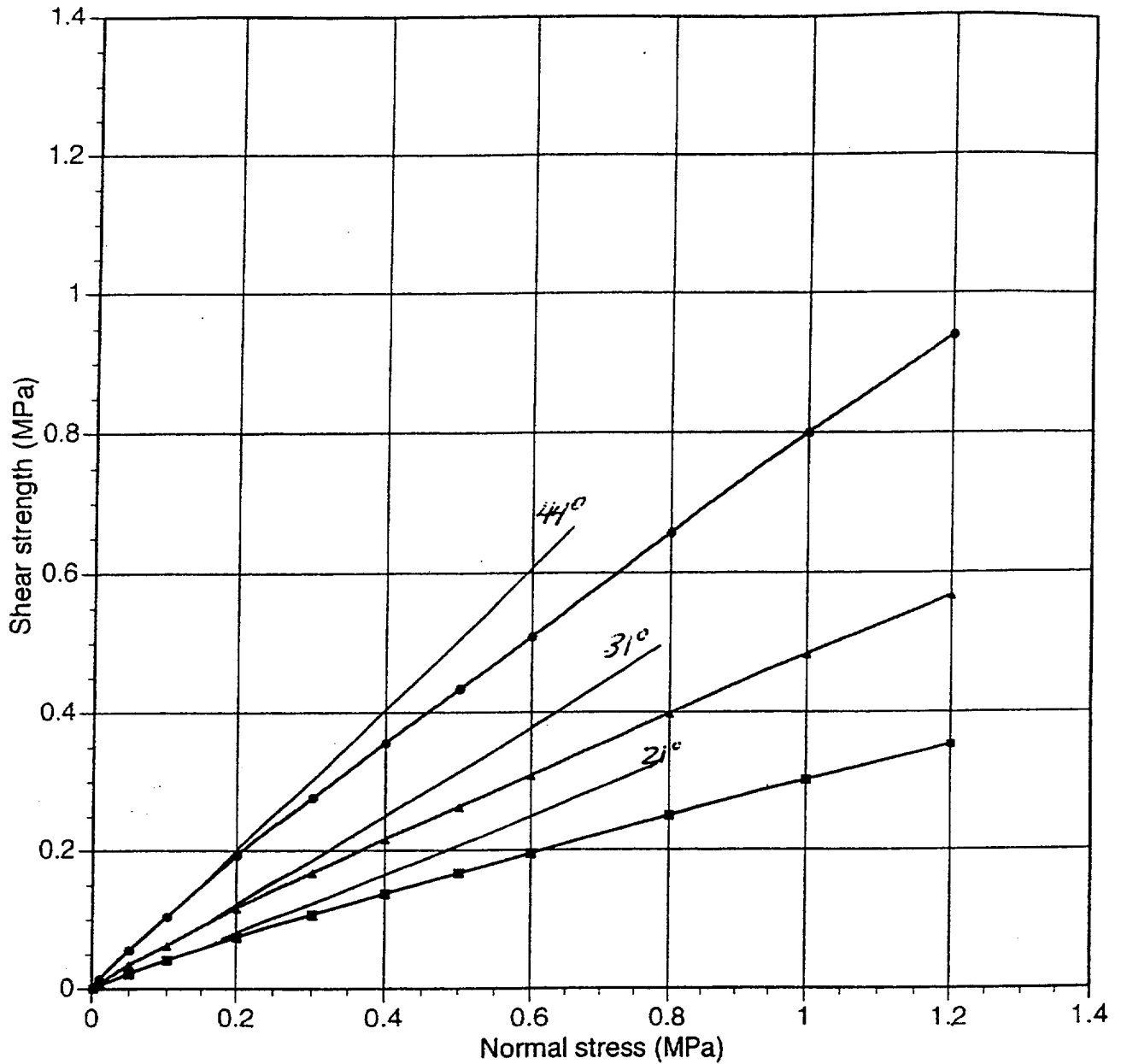


36° Tangent line drawn tangent to the curve at the midpoint of normal stress range (0 to 0.15 MPa).

Note: Upper and lower bounds for JRC and JCS represent one standard deviation above and below the mean values, respectively. Upper and lower bounds for basal friction angle are based on a range of strength envelopes for clean joints (upper bound), clay-coated joints (lower bound), and combination of both (mean). Curves compiled from Attachment 3, pages 53 - 55.

Figure 20-5. Sandstone Joint Shear Strength Curve D

Comparison of Barton bedding strength- Sandstone (Tof_{b-2})



Lower bound

 Upper bound

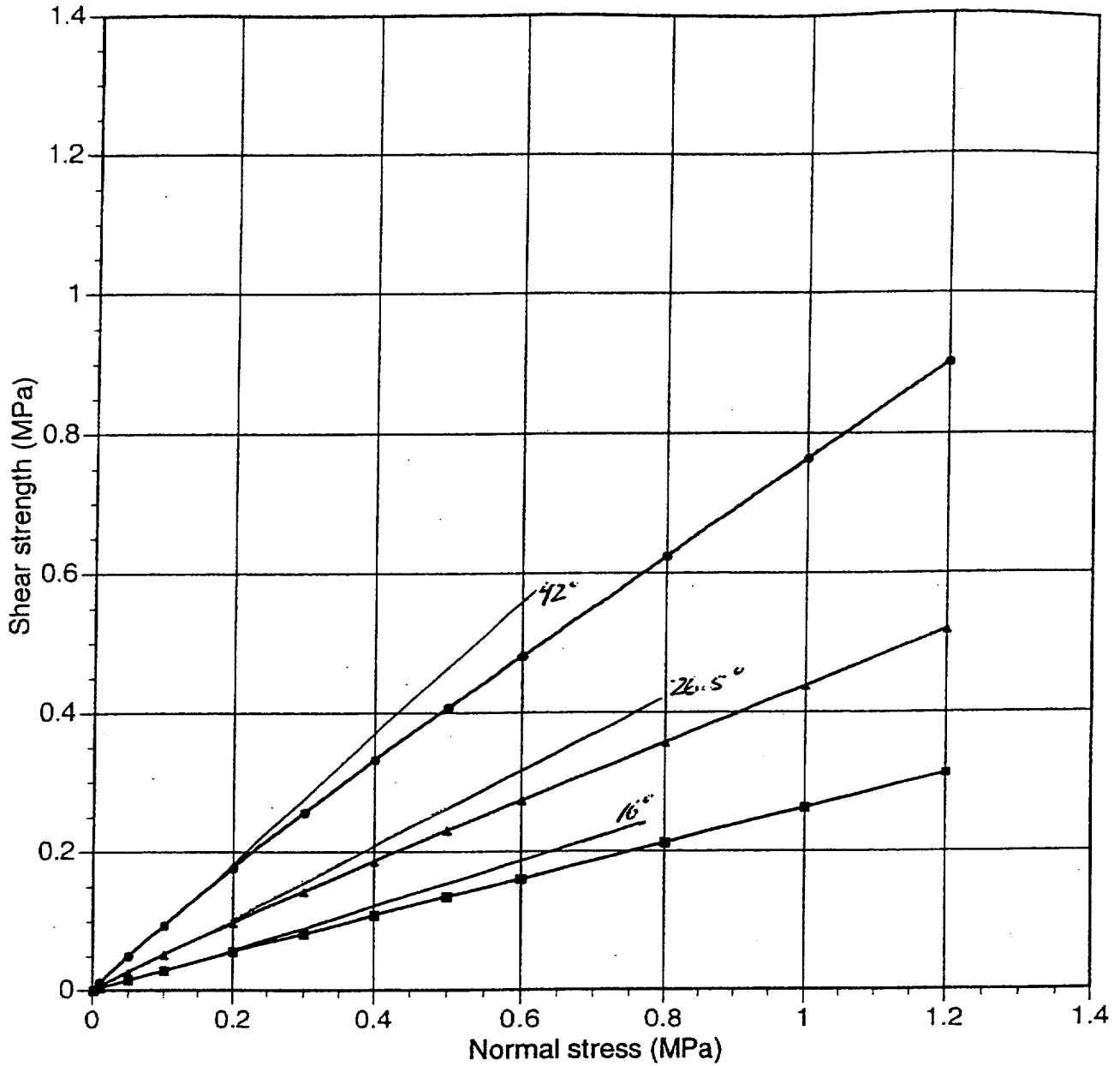
 Mean

36° Tangent line drawn tangent to the curve at the midpoint of normal stress range (0 to 0.15 MPa).

Note: Upper and lower bounds for JRC and JCS represent one standard deviation above and below the mean values, respectively. Upper and lower bounds for basal friction angle are based on a range of strength envelopes for clean joints (upper bound), clay-coated joints (lower bound), and combination of both (mean). Curves compiled from Attachment 3, pages 56- 58.

Figure 20-6. Sandstone Bedding Shear Strength Curve E

Comparison of Barton fault strength- Sandstone (Tof_{b-2})



Lower bound

 Upper bound

 Mean

Note: Upper and lower bounds for JRC and JCS represent one standard deviation above and below the mean values, respectively. Upper and lower bounds for basal friction angle are based on a range of strength envelopes for clean joints (upper bound), clay-coated joints (lower bound), and combination of both (mean). Curves compiled from Attachment 3, pages 59 - 61.

36° Tangent line drawn tangent to the curve at the midpoint of normal stress range (0 to 0.15 MPa).

Figure 20-7. Sandstone Faults Shear Strength Curve F

ATTACHMENT 1
Rock Engineering Course Notes, Chapter 4
(version dated Nov. 27, 2000)
E. Hoek, 2000

Downloaded from Rocscience website (www.rocscience.com) June 28, 2001

Shear strength of discontinuities

4.1 Introduction

All rock masses contain discontinuities such as bedding planes, joints, shear zones and faults. At shallow depth, where stresses are low, failure of the intact rock material is minimal and the behaviour of the rock mass is controlled by sliding on the discontinuities. In order to analyse the stability of this system of individual rock blocks, it is necessary to understand the factors that control the shear strength of the discontinuities which separate the blocks. These questions are addressed in the discussion that follows.

4.2 Shear strength of planar surfaces

Suppose that a number of samples of a rock are obtained for shear testing. Each sample contains a through-going bedding plane that is cemented; in other words, a tensile force would have to be applied to the two halves of the specimen in order to separate them. The bedding plane is absolutely planar, having no surface irregularities or undulations. As illustrated in Figure 4.1, in a shear test each specimen is subjected to a stress σ_n normal to the bedding plane, and the shear stress τ , required to cause a displacement δ , is measured.

The shear stress will increase rapidly until the peak strength is reached. This corresponds to the sum of the strength of the cementing material bonding the two halves of the bedding plane together and the frictional resistance of the matching surfaces. As the displacement continues, the shear stress will fall to some residual value that will then remain constant, even for large shear displacements.

Plotting the peak and residual shear strengths for different normal stresses results in the two lines illustrated in Figure 4.1. For planar discontinuity surfaces the experimental points will generally fall along straight lines. The peak strength line has a slope of ϕ and an intercept of c on the shear strength axis. The residual strength line has a slope of ϕ_r .

The relationship between the peak shear strength τ_p and the normal stress σ_n can be represented by the Mohr-Coulomb equation:

$$\tau_p = c + \sigma_n \tan \phi \quad (4.1)$$

where c is the cohesive strength of the cemented surface and ϕ is the angle of friction.

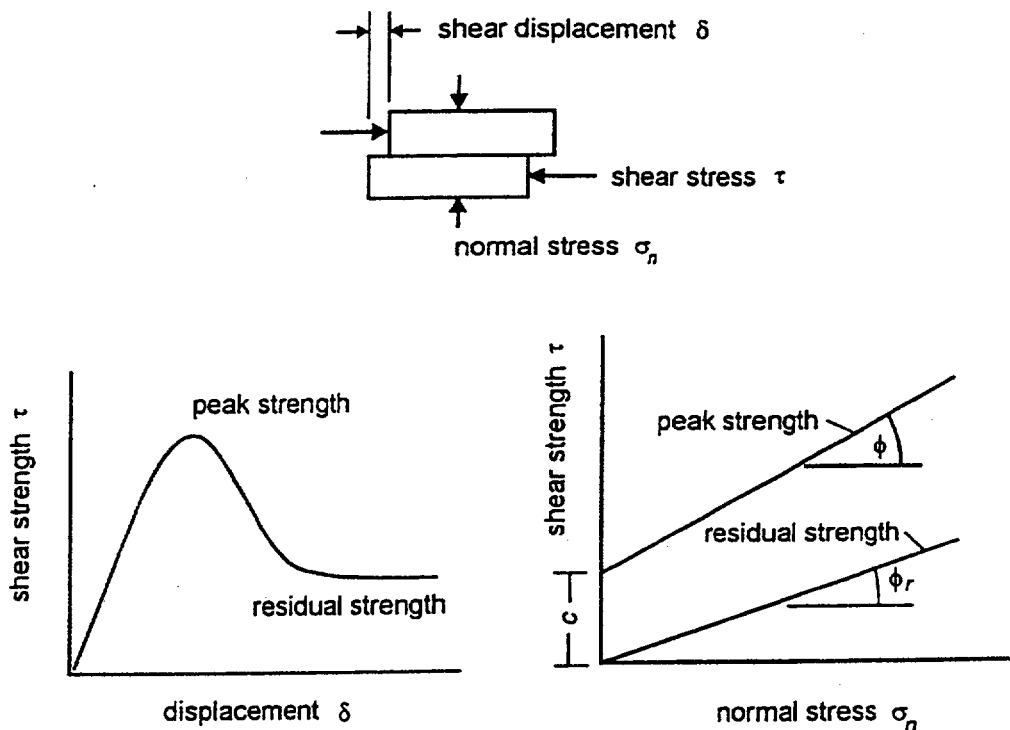


Figure 4.1: Shear testing of discontinuities

In the case of the residual strength, the cohesion c has dropped to zero and the relationship between ϕ_r and σ_n can be represented by:

$$\tau_r = \sigma_n \tan \phi_r \tag{4.2}$$

where ϕ_r is the residual angle of friction.

This example has been discussed in order to illustrate the physical meaning of the term cohesion, a soil mechanics term, which has been adopted by the rock mechanics community. In shear tests on soils, the stress levels are generally an order of magnitude lower than those involved in rock testing and the cohesive strength of a soil is a result of the adhesion of the soil particles. In rock mechanics, true cohesion occurs when cemented surfaces are sheared. However, in many practical applications, the term cohesion is used for convenience and it refers to a mathematical quantity related to surface roughness, as discussed in a later section. Cohesion is simply the intercept on the τ axis at zero normal stress.

The basic friction angle ϕ_b is a quantity that is fundamental to the understanding of the shear strength of discontinuity surfaces. This is approximately equal to the residual friction angle ϕ_r but it is generally measured by testing sawn or ground rock surfaces. These tests, which can be carried out on surfaces as small as 50 mm x 50 mm, will produce a straight line plot defined by the equation :

$$\tau_r = \sigma_n \tan \phi_b \tag{4.3}$$

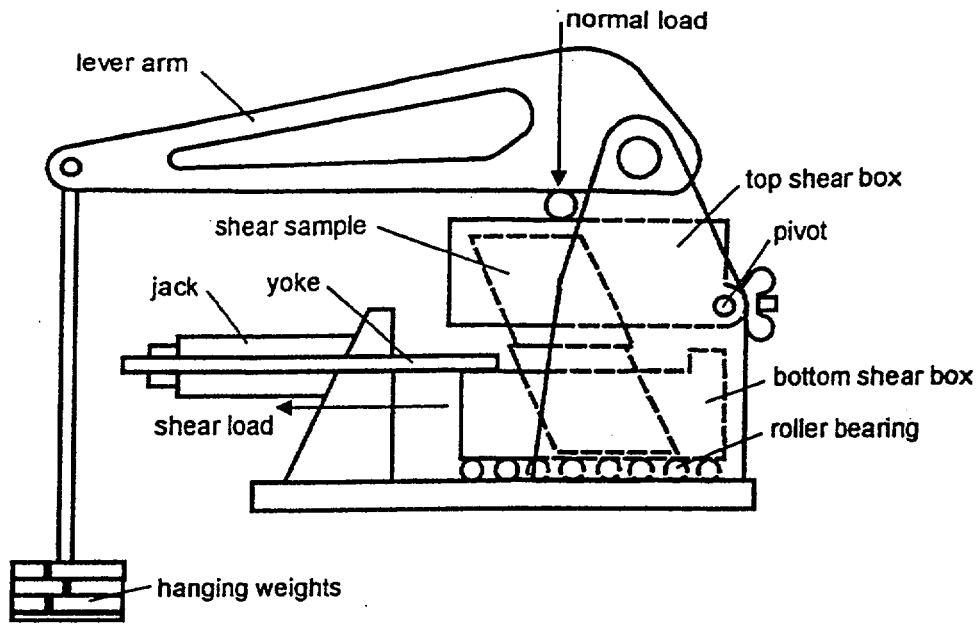


Figure 4.2: Diagrammatic section through shear machine used by Hencher and Richards (1982).

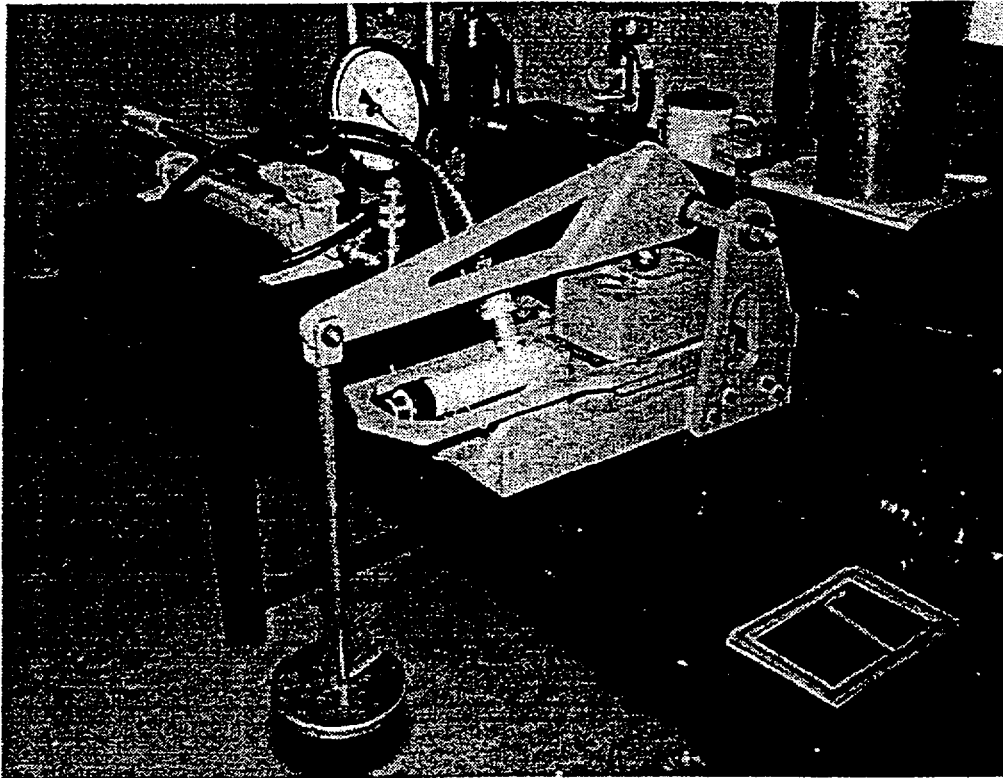


Figure 4.3: Shear machine of the type used by Hencher and Richards (1982) for measurement of the shear strength of sheet joints in Hong Kong granite.

A typical shear testing machine, which can be used to determine the basic friction angle ϕ_b is illustrated in Figures 4.2 and 4.3. This is a very simple machine and the use of a mechanical lever arm ensures that the normal load on the specimen remains constant throughout the test. This is an important practical consideration since it is difficult to maintain a constant normal load in hydraulically or pneumatically controlled systems and this makes it difficult to interpret test data.

Note that it is important that, in setting up the specimen, great care has to be taken to ensure that the shear surface is aligned accurately in order to avoid the need for an additional angle correction.

Most shear strength determinations today are carried out by determining the basic friction angle, as described above, and then making corrections for surface roughness as discussed in the following sections of this chapter. In the past there was more emphasis on testing full scale discontinuity surfaces, either in the laboratory or in the field. There are a significant number of papers in the literature of the 1960s and 1970s describing large and elaborate in situ shear tests, many of which were carried out to determine the shear strength of weak layers in dam foundations. However, the high cost of these tests together with the difficulty of interpreting the results has resulted in a decline in the use of these large scale tests and they are seldom seen today.

The author's opinion is that it makes both economical and practical sense to carry out a number of small scale laboratory shear tests, using equipment such as that illustrated in Figures 4.2 and 4.3, to determine the basic friction angle. The roughness component which is then added to this basic friction angle to give the effective friction angle is a number which is site specific and scale dependent and is best obtained by visual estimates in the field. Practical techniques for making these roughness angle estimates are described on the following pages.

4.3 Shear strength of rough surfaces

A natural discontinuity surface in hard rock is never as smooth as a sawn or ground surface of the type used for determining the basic friction angle. The undulations and asperities on a natural joint surface have a significant influence on its shear behaviour. Generally, this surface roughness increases the shear strength of the surface, and this strength increase is extremely important in terms of the stability of excavations in rock.

Patton (1966) demonstrated this influence by means of an experiment in which he carried out shear tests on 'saw-tooth' specimens such as the one illustrated in Figure 4.4. Shear displacement in these specimens occurs as a result of the surfaces moving up the inclined faces, causing dilation (an increase in volume) of the specimen.

The shear strength of Patton's saw-tooth specimens can be represented by:

$$\tau = \sigma_n \tan(\phi_b + i) \quad (4.4)$$

where ϕ_b is the basic friction angle of the surface and
 i is the angle of the saw-tooth face.

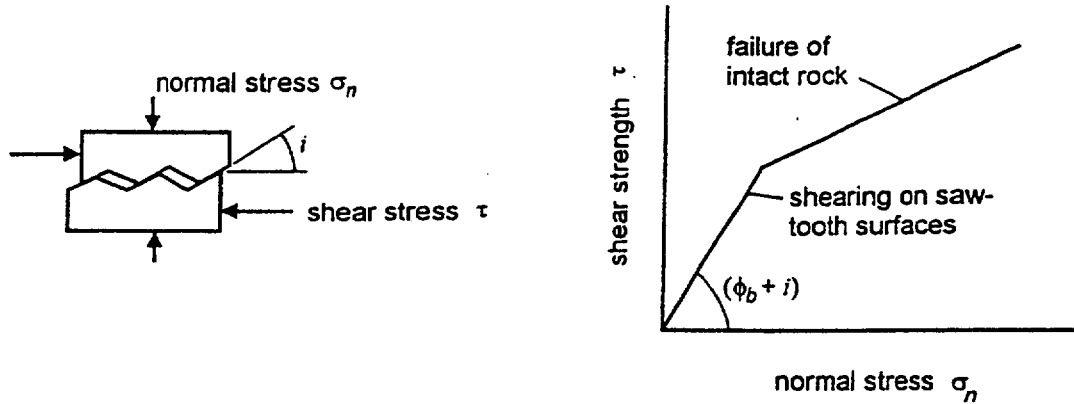


Figure 4.4: Patton's experiment on the shear strength of saw-tooth specimens.

4.4 Barton's estimate of shear strength

Equation (4.4) is valid at low normal stresses where shear displacement is due to sliding along the inclined surfaces. At higher normal stresses, the strength of the intact material will be exceeded and the teeth will tend to break off, resulting in a shear strength behaviour which is more closely related to the intact material strength than to the frictional characteristics of the surfaces.

While Patton's approach has the merit of being very simple, it does not reflect the reality that changes in shear strength with increasing normal stress are gradual rather than abrupt. Barton and his co-workers (1973, 1976, 1977, 1990) studied the behaviour of natural rock joints and have proposed that equation (4.4) can be re-written as:

$$\tau = \sigma_n \tan \left(\phi_b + JRC \log_{10} \left(\frac{JCS}{\sigma_n} \right) \right) \quad (4.5)$$

where JRC is the joint roughness coefficient and JCS is the joint wall compressive strength.

4.5 Field estimates of JRC

The joint roughness coefficient JRC is a number that can be estimated by comparing the appearance of a discontinuity surface with standard profiles published by Barton and others. One of the most useful of these profile sets was published by Barton and Choubey (1977) and is reproduced in Figure 4.2.

The appearance of the discontinuity surface is compared visually with the profiles shown and the JRC value corresponding to the profile which most closely matches that of the discontinuity surface is chosen. In the case of small scale laboratory specimens, the scale of the surface roughness will be approximately the same as that of the profiles illustrated. However, in the field the length of the surface of interest may be several metres or even tens of metres and the JRC value must be estimated for the full scale surface.

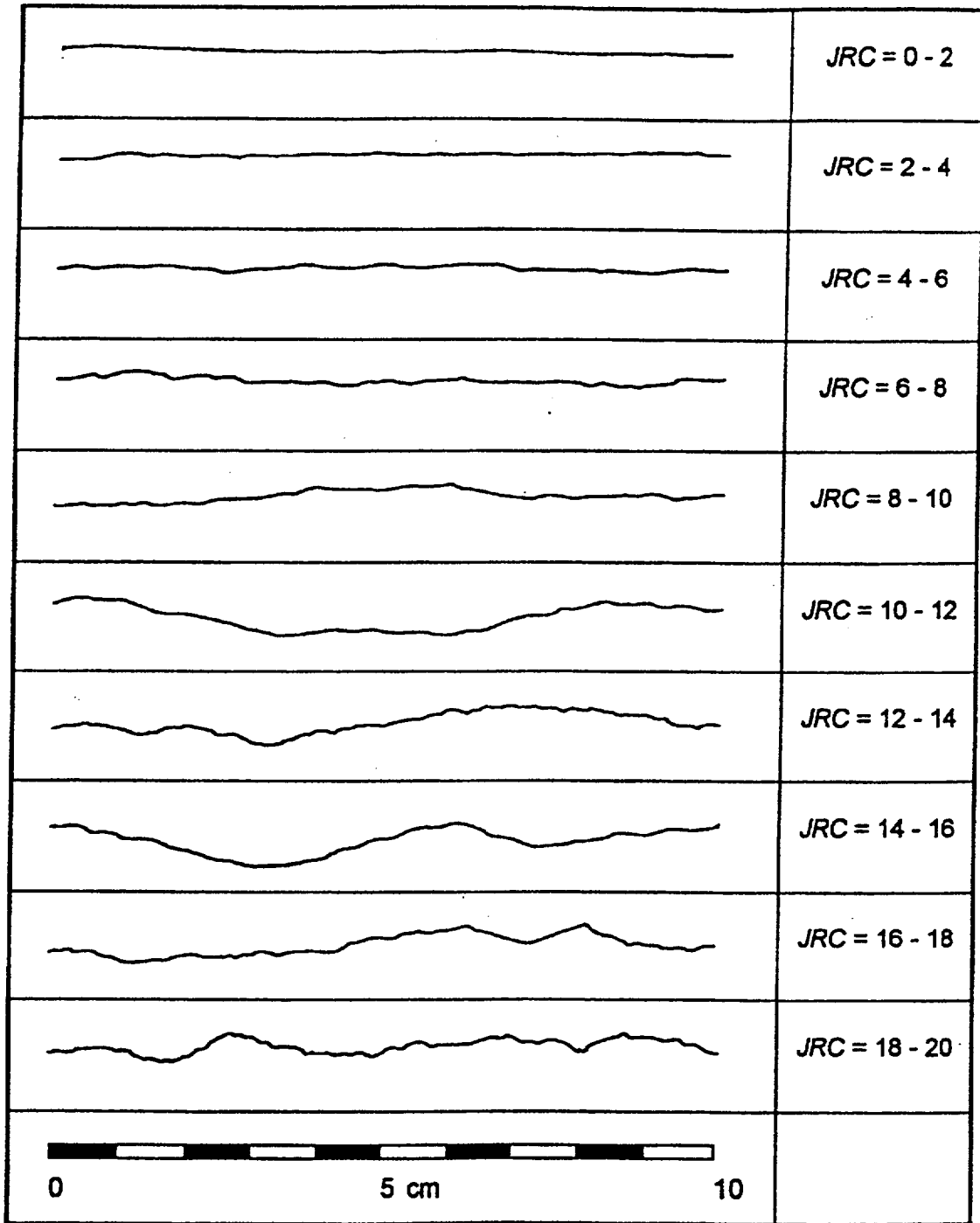


Figure 4.2: Roughness profiles and corresponding JRC values (After Barton and Choubey 1977).

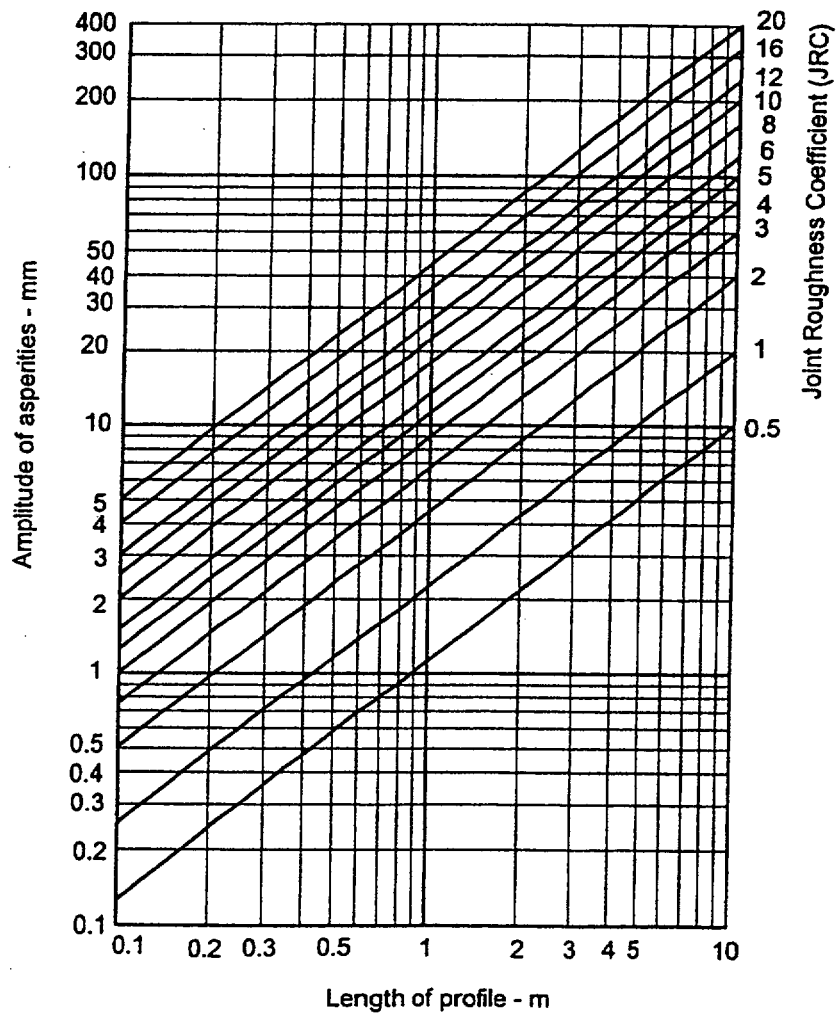
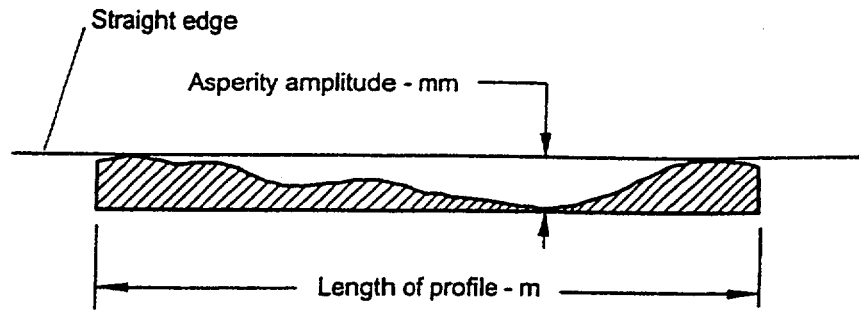


Figure 4.6: Alternative method for estimating *JRC* from measurements of surface roughness amplitude from a straight edge (Barton 1982).

4.6 Field estimates of JCS

Suggested methods for estimating the joint wall compressive strength were published by the ISRM (1978). The use of the Schmidt rebound hammer for estimating joint wall compressive strength was proposed by Deere and Miller (1966), as illustrated in Figure 4.7.

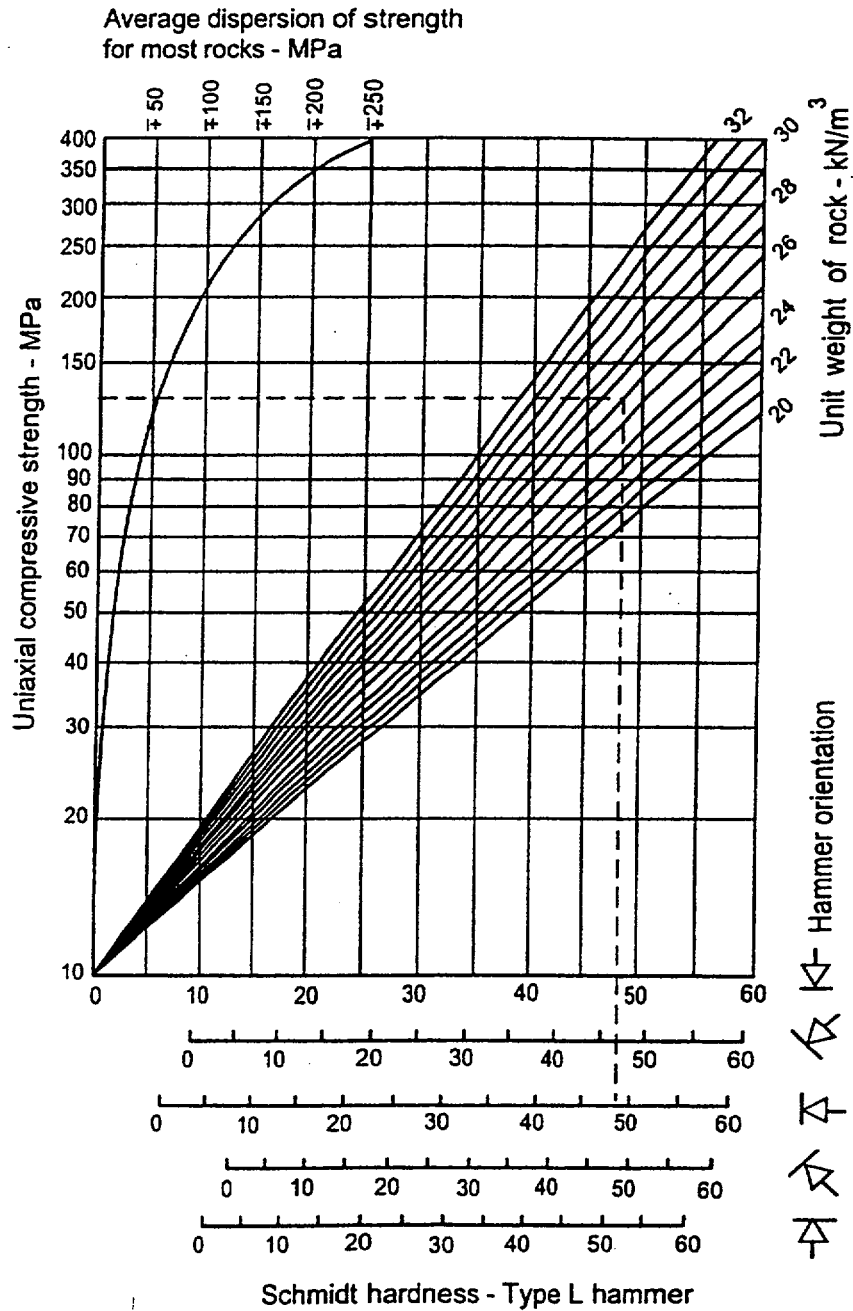


Figure 4.7: Estimate of joint wall compressive strength from Schmidt hardness.

4.7 Influence of scale on *JRC* and *JCS*

On the basis of extensive testing of joints, joint replicas, and a review of literature, Barton and Bandis (1982) proposed the scale corrections for *JRC* defined by the following relationship:

$$JRC_n = JRC_o \left(\frac{L_n}{L_o} \right)^{-0.02JRC_o} \quad (4.6)$$

where JRC_o , and L_o (length) refer to 100 mm laboratory scale samples and JRC_n , and L_n refer to in situ block sizes.

Because of the greater possibility of weaknesses in a large surface, it is likely that the average joint wall compressive strength (*JCS*) decreases with increasing scale. Barton and Bandis (1982) proposed the scale corrections for *JCS* defined by the following relationship:

$$JCS_n = JCS_o \left(\frac{L_n}{L_o} \right)^{-0.03JRC_o} \quad (4.7)$$

where JCS_o and L_o (length) refer to 100 mm laboratory scale samples and JCS_n and L_n refer to in situ block sizes.

4.8 Shear strength of filled discontinuities

The discussion presented in the previous sections has dealt with the shear strength of discontinuities in which rock wall contact occurs over the entire length of the surface under consideration. This shear strength can be reduced drastically when part or all of the surface is not in intimate contact, but covered by soft filling material such as clay gouge. For planar surfaces, such as bedding planes in sedimentary rock, a thin clay coating will result in a significant shear strength reduction. For a rough or undulating joint, the filling thickness has to be greater than the amplitude of the undulations before the shear strength is reduced to that of the filling material.

A comprehensive review of the shear strength of filled discontinuities was prepared by Barton (1974) and a summary of the shear strengths of typical discontinuity fillings, based on Barton's review, is given in Table 4.1.

Where a significant thickness of clay or gouge fillings occurs in rock masses and where the shear strength of the filled discontinuities is likely to play an important role in the stability of the rock mass, it is strongly recommended that samples of the filling be sent to a soil mechanics laboratory for testing.

Table 4.1: Shear strength of filled discontinuities and filling materials (After Barton 1974)

Rock	Description	Peak c' (MPa)	Peak ϕ°	Residual c' (MPa)	Residual ϕ°
Basalt	Clayey basaltic breccia, wide variation from clay to basalt content	0.24	42		
Bentonite	Bentonite seam in chalk	0.015	7.5		
	Thin layers	0.09-0.12	12-17		
	Triaxial tests	0.06-0.1	9-13		
Bentonitic shale	Triaxial tests	0-0.27	8.5-29		
	Direct shear tests			0.03	8.5
Clays	Over-consolidated, slips, joints and minor shears	0-0.18	12-18.5	0-0.003	10.5-16
Clay shale	Triaxial tests	0.06	32		
	Stratification surfaces			0	19-25
Coal measure rocks	Clay mylonite seams, 10 to 25 mm	0.012	16	0	11-11.5
Dolomite	Altered shale bed, \pm 150 mm thick	0.04	14.5	0.02	17
Diorite, granodiorite and porphyry	Clay gouge (2% clay, PI = 17%)	0	26.5		
Granite	Clay filled faults	0-0.1	24-45		
	Sandy loam fault filling	0.05	40		
	Tectonic shear zone, schistose and broken granites, disintegrated rock and gouge	0.24	42		
Greywacke	1-2 mm clay in bedding planes			0	21
Limestone	6 mm clay layer			0	13
	10-20 mm clay fillings	0.1	13-14		
	<1 mm clay filling	0.05-0.2	17-21		
Limestone, marl and lignites	Interbedded lignite layers	0.08	38		
	Lignite/marl contact	0.1	10		
Limestone	Marlaceous joints, 20 mm thick	0	25	0	15-24
Lignite	Layer between lignite and clay	0.014-0.03	15-17.5		
Montmorillonite	80 mm seams of bentonite (montmorillonite) clay in chalk	0.36	14	0.08	11
Bentonite clay		0.016-0.02	7.5-11.5		
Schists, quartzites and siliceous schists	100-15- mm thick clay filling	0.03-0.08	32		
	Stratification with thin clay	0.61-0.74	41		
	Stratification with thick clay	0.38	31		
Slates	Finely laminated and altered	0.05	33		
Quartz / kaolin / pyrolusite	Remoulded triaxial tests	0.042-0.09	36-38		

4.9 Influence of water pressure

When water pressure is present in a rock mass, the surfaces of the discontinuities are forced apart and the normal stress σ_n is reduced. Under steady state conditions, where there is sufficient time for the water pressures in the rock mass to reach equilibrium, the reduced normal stress is defined by $\sigma_n' = (\sigma_n - u)$, where u is the water pressure. The reduced normal stress σ_n' is usually called the effective normal stress, and it can be used in place of the normal stress term σ_n in all of the equations presented in previous sections of this chapter.

4.10 Instantaneous cohesion and friction

Due to the historical development of the subject of rock mechanics, many of the analyses, used to calculate factors of safety against sliding, are expressed in terms of the Mohr-Coulomb cohesion (c) and friction angle (ϕ), defined in Equation 4.1. Since the 1970s it has been recognised that the relationship between shear strength and normal stress is more accurately represented by a non-linear relationship such as that proposed by Barton (1973). However, because this relationship (e.g. Equation 4.5) is not expressed in terms of c and ϕ , it is necessary to devise some means for estimating the equivalent cohesive strengths and angles of friction from relationships such as those proposed by Barton.

Figure 4.8 gives definitions of the *instantaneous cohesion* c_i and the *instantaneous friction angle* ϕ_i for a normal stress of σ_n . These quantities are given by the intercept and the inclination, respectively, of the tangent to the non-linear relationship between shear strength and normal stress. These quantities may be used for stability analyses in which the Mohr-Coulomb failure criterion (Equation 4.1) is applied, provided that the normal stress σ_n is reasonably close to the value used to define the tangent point.

In a typical practical application, a spreadsheet program can be used to solve Equation 4.5 and to calculate the instantaneous cohesion and friction values for a range of normal stress values. A portion of such a spreadsheet is illustrated in Figure 4.9.

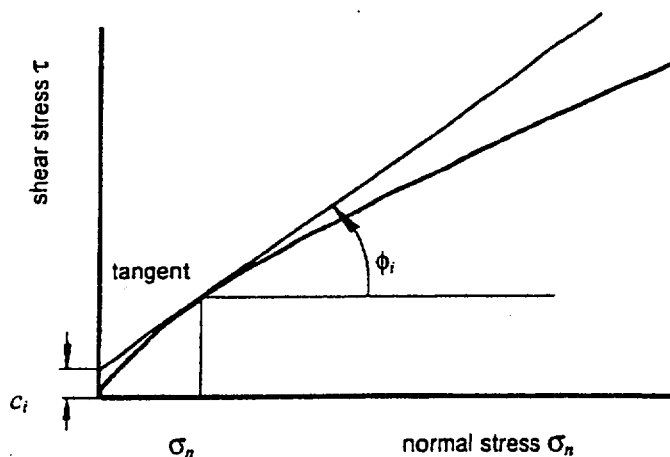


Figure 4.8: Definition of instantaneous cohesion c_i and instantaneous friction angle ϕ_i for a non-linear failure criterion.

Barton shear failure criterion*Input parameters:*

Basic friction angle (PHIB) - degrees	29
Joint roughness coefficient (JRC)	16.9
Joint compressive strength (JCS)	96
Minimum normal stress (SIGNMIN)	0.360

Normal stress (SIGN) MPa	Shear strength (TAU) MPa	dTAU dSIGN (DTDS)	Friction angle (PHI) degrees	Cohesive strength (COH) MPa
0.360	0.989	1.652	58.82	0.394
0.720	1.538	1.423	54.91	0.513
1.440	2.476	1.213	50.49	0.730
2.880	4.073	1.030	45.85	1.107
5.759	6.779	0.872	41.07	1.760
11.518	11.344	0.733	36.22	2.907
23.036	18.973	0.609	31.33	4.953
46.073	31.533	0.496	26.40	8.666

Cell formulae:

```

SIGNMIN = 10^(LOG(JCS)-((70-PHIB)/JRC))
TAU = SIGN*TAN((PHIB+JRC*LOG(JCS/SIGN))*PI()/180)

DTDS = TAN((JRC*LOG(JCS/SIGN)+PHIB)*PI()/180)-(JRC/LN(10))
      *(TAN((JRC*LOG(JCS/SIGN)+PHIB)*PI()/180)^2+1)*PI()/180

PHI = ATAN(DTDS)*180/PI()
COH = TAU-SIGN*DTDS

```

Figure 4.9 Printout of spreadsheet cells and formulae used to calculate shear strength, instantaneous friction angle and instantaneous cohesion for a range of normal stresses.

Note that equation 4.5 is not valid for $\sigma_n = 0$ and it ceases to have any practical meaning for $\phi_b + JRC \log_{10}(JCS / \sigma_n) > 70^\circ$. This limit can be used to determine a minimum value for σ_n . An upper limit for σ_n is given by $\sigma_n = JCS$.

In the spreadsheet shown in Figure 4.9, the instantaneous friction angle ϕ_i , for a normal stress of σ_n , has been calculated from the relationship

$$\phi_i = \arctan\left(\frac{\partial \tau}{\partial \sigma_n}\right) \quad (4.8)$$

$$\frac{\partial \tau}{\partial \sigma_n} = \tan \left(JRC \log_{10} \frac{JCS}{\sigma_n} + \phi_b \right) - \frac{\pi JRC}{180 \ln 10} \left[\tan^2 \left(JRC \log_{10} \frac{JCS}{\sigma_n} + \phi_b \right) + 1 \right] \quad (4.9)$$

The instantaneous cohesion c_i is calculated from:

$$c_i = \tau - \sigma_n \tan \phi_i \quad (4.10)$$

In choosing the values of c_i and ϕ_i for use in a particular application, the average normal stress σ_n acting on the discontinuity planes should be estimated and used to determine the appropriate row in the spreadsheet. For many practical problems in the field, a single average value of σ_n will suffice but, where critical stability problems are being considered, this selection should be made for each important discontinuity surface.

ATTACHMENT 2

Barton Spreadsheet Verification Runs

Barton shear failure criterion

Input

Input parameters:	
Basic friction angle (PHIB) - degrees	29
Joint roughness coefficient (JRC)	16.9
Joint compressive strength (JCS)	96
Minimum normal stress (SIGNMIN)	0.360

Verification Run
Sample Problems
Hocak, 2000

Normal stress (SIGN) MPa	Shear strength (TAU) MPa	dTAU dSIGN (DTDS)	Friction angle (PHI) degrees	Cohesive strength (COH) MPa
0.360	0.989	1.652	58.82	0.394
0.720	1.538	1.423	54.91	0.513
1.440	2.476	1.213	50.49	0.730
2.880	4.073	1.030	45.85	1.107
5.759	6.779	0.872	41.07	1.760
11.518	11.344	0.733	36.22	2.907
23.036	18.973	0.609	31.33	4.953
46.073	31.533	0.496	26.40	8.666

Cell formulae:

Output

$$\text{SIGNMIN} = 10^{((70-\text{PHIB})/\text{JRC})}$$

$$\text{TAU} = \text{SIGN} * \text{TAN}(((\text{PHIB} + \text{JRC} * \text{LOG}(\text{JCS}/\text{SIGN})) * \text{PI}()) / 180)$$

$$\text{DTDS} = \text{TAN}((\text{JRC} * \text{LOG}(\text{JCS}/\text{SIGN}) + \text{PHIB}) * \text{PI}() / 180) - (\text{JRC} / \text{LN}(10)) * (\text{TAN}((\text{JRC} * \text{LOG}(\text{JCS}/\text{SIGN}) + \text{PHIB}) * \text{PI}() / 180)^2 + 1) * \text{PI}() / 180$$

$$\text{PHI} = \text{ATAN}(\text{DTDS}) * 180 / \text{PI}()$$

$$\text{COH} = \text{TAU} - \text{SIGN} * \text{DTDS}$$

Figure 4.9 Printout of spreadsheet cells and formulae used to calculate shear strength, instantaneous friction angle and instantaneous cohesion for a range of normal stresses.

Note that equation 4.5 is not valid for $\sigma_n = 0$ and it ceases to have any practical meaning for $\phi_b + \text{JRC} \log_{10}(\text{JCS} / \sigma_n) > 70^\circ$. This limit can be used to determine a minimum value for σ_n . An upper limit for σ_n is given by $\sigma_n = \text{JCS}$.

In the spreadsheet shown in Figure 4.9, the instantaneous friction angle ϕ_i , for a normal stress of σ_n , has been calculated from the relationship

$$\phi_i = \arctan\left(\frac{\partial \tau}{\partial \sigma_n}\right) \tag{4.8}$$

Verification Run
Jib Excel Spreadsheet

BARTON SHEAR FAILURE CRITERION (from Hoek, 1998) BtrnVerifyRun.Ro

**ISFSI BORROW SITE - VERIFICATION RUN, HOEK (2000) PAGE 71
TOFB-1 - BEDDING LOW**

INPUT FIELDS

Basic Friction Angle (PHIB) - degrees
Joint Roughness Coeff. (JRC)
Joint Compressive Strength (JCS) - MPA
Min. Normal Stress (SIGNMIN) - MPA

29.0
16.9
96.0

Input

0.360 calculated min. value

OUTPUT

	Normal Stress (SIGN) MPA	Shear Strength (TAU) MPA	dTAU/dSIGN (DTDS)	Friction Angle (PHI) degrees	Cohesive Strength (COH) MPA
Input, or F10	0.360	0.989	1.652	58.82	0.394
	0.720	1.538	1.423	54.91	0.513
	1.440	2.477	1.213	50.49	0.730
	2.880	4.073	1.030	45.85	1.107
	5.759	6.779	0.872	41.07	1.760
	11.518	11.344	0.733	36.22	2.907
	23.036	18.973	0.609	31.33	4.953
	46.073	31.533	0.496	26.40	8.667

Output

REFERENCE: Hoek, 2000

ATTACHMENT 3
ISFSI Site Barton Shear Strength Runs

BARTON SHEAR FAILURE CRITERION

**ISFSI BORROW SITE - DOLOMITE JOINTS
TOFB-1 - JOINTS LOW**

INPUT FIELDS

Basic Friction Angle (PHIB) - degrees	14.0
Joint Roughness Coeff. (JRC)	3.3
Joint Compressive Strength (JCS) - MPA	4.3
Min. Normal Stress (SIGNMIN) - MPA	0.000 calculated min. value

OUTPUT

	Normal Stress (SIGN) MPA	Shear Strength (TAU) MPA	dTAU/dSIGN (DTDS)	Friction Angle (PHI) degrees	Cohesive Strength (COH) MPA
Input, or F10	0.001	0.000	0.457	24.57	0.000
	0.010	0.004	0.389	21.26	0.000
	0.050	0.019	0.343	18.95	0.001
	0.100	0.035	0.324	17.96	0.003
	0.200	0.067	0.305	16.96	0.006
	0.300	0.096	0.294	16.38	0.008
	0.400	0.125	0.286	15.97	0.011
	0.500	0.154	0.280	15.64	0.014
	0.600	0.182	0.275	15.38	0.016
	0.800	0.236	0.267	14.97	0.022
	1.000	0.289	0.261	14.65	0.027
	1.200	0.340	0.257	14.39	0.033

BARTON SHEAR FAILURE CRITERION

**ISFSI BORROW SITE - DOLOMITE JOINTS
TOFB-1 - JOINTS MEAN**

INPUT FIELDS

Basic Friction Angle (PHIB) - degrees	26.0
Joint Roughness Coeff. (JRC)	5.6
Joint Compressive Strength (JCS) - MPA	8.0
Min. Normal Stress (SIGNMIN) - MPA	0.000 calculated min. value

OUTPUT

	Normal Stress (SIGN) MPA	Shear Strength (TAU) MPA	dTAU/dSIGN (DTDS)	Friction Angle (PHI) degrees	Cohesive Strength (COH) MPA
Input, or F10	0.001	0.001	1.011	45.31	0.000
	0.010	0.009	0.831	39.73	0.001
	0.050	0.040	0.722	35.83	0.003
	0.100	0.074	0.678	34.15	0.007
	0.200	0.140	0.636	32.47	0.013
	0.300	0.202	0.612	31.48	0.019
	0.400	0.263	0.596	30.79	0.024
	0.500	0.322	0.583	30.24	0.030
	0.600	0.379	0.573	29.80	0.036
	0.800	0.492	0.557	29.10	0.047
	1.000	0.602	0.544	28.56	0.058
	1.200	0.710	0.534	28.12	0.069

BARTON SHEAR FAILURE CRITERION

ISFSI BORROW SITE - DOLOMITE JOINTS TOFB-1 - JOINTS HIGH

INPUT FIELDS

Basic Friction Angle (PHIB) - degrees	38	
Joint Roughness Coeff. (JRC)	7.9	
Joint Compressive Strength (JCS) - MPA	11.8	
Min. Normal Stress (SIGNMIN) - MPA		0.001 calculated min. value

OUTPUT

	Normal Stress (SIGN) MPA	Shear Strength (TAU) MPA	dTAU/dSIGN (DTDS)	Friction Angle (PHI) degrees	Cohesive Strength (COH) MPA
Input, or F10	0.001	0.003	2.252	66.06	0.001
	0.010	0.019	1.626	58.40	0.003
	0.050	0.076	1.326	52.98	0.010
	0.100	0.140	1.219	50.63	0.018
	0.200	0.256	1.122	48.28	0.032
	0.300	0.365	1.069	46.90	0.045
	0.400	0.470	1.033	45.93	0.057
	0.500	0.572	1.006	45.17	0.069
	0.600	0.672	0.984	44.55	0.081
	0.800	0.865	0.951	43.57	0.104
	1.000	1.053	0.926	42.81	0.126
	1.200	1.236	0.906	42.19	0.148

BARTON SHEAR FAILURE CRITERION

**ISFSI BORROW SITE - DOLOMITE BEDDING
TOFB-1 - BEDDING LOW**

INPUT FIELDS

Basic Friction Angle (PHIB) - degrees	14.0
Joint Roughness Coeff. (JRC)	3.2
Joint Compressive Strength (JCS) - MPA	4.3
Min. Normal Stress (SIGNMIN) - MPA	0.000 calculated min. value

OUTPUT

	Normal Stress (SIGN) MPA	Shear Strength (TAU) MPA	dTAU/dSIGN (DTDS)	Friction Angle (PHI) degrees	Cohesive Strength (COH) MPA
Input, or F10	0.001	0.000	0.449	24.16	0.000
	0.010	0.004	0.383	20.98	0.000
	0.050	0.018	0.340	18.76	0.001
	0.100	0.035	0.321	17.80	0.003
	0.200	0.066	0.303	16.85	0.005
	0.300	0.096	0.292	16.29	0.008
	0.400	0.124	0.285	15.89	0.011
	0.500	0.153	0.279	15.58	0.013
	0.600	0.180	0.274	15.33	0.016
	0.800	0.234	0.267	14.93	0.021
	1.000	0.287	0.261	14.62	0.026
	1.200	0.339	0.256	14.37	0.031

BARTON SHEAR FAILURE CRITERION

ISFSI BORROW SITE - DOLOMITE BEDDING TOFB-1 - BEDDING MEAN

INPUT FIELDS

Basic Friction Angle (PHIB) - degrees	26.0	
Joint Roughness Coeff. (JRC)	4.4	
Joint Compressive Strength (JCS) - MPA	8.0	
Min. Normal Stress (SIGNMIN) - MPA		0.000 calculated min. value

OUTPUT

	Normal Stress (SIGN) MPA	Shear Strength (TAU) MPA	dTAU/dSIGN (DTDS)	Friction Angle (PHI) degrees	Cohesive Strength (COH) MPA
Input, or F10	0.001	0.001	0.875	41.20	0.000
	0.010	0.008	0.748	36.81	0.001
	0.050	0.036	0.668	33.74	0.003
	0.100	0.068	0.635	32.42	0.005
	0.200	0.130	0.603	31.10	0.009
	0.300	0.189	0.585	30.32	0.014
	0.400	0.247	0.572	29.77	0.018
	0.500	0.304	0.562	29.35	0.023
	0.600	0.360	0.554	29.00	0.027
	0.800	0.469	0.542	28.45	0.036
	1.000	0.577	0.532	28.03	0.044
	1.200	0.682	0.525	27.68	0.053

BARTON SHEAR FAILURE CRITERION

ISFSI BORROW SITE - DOLOMITE BEDDING TOFB-1 - BEDDING HIGH

INPUT FIELDS

Basic Friction Angle (PHIB) - degrees	38.0
Joint Roughness Coeff. (JRC)	5.6
Joint Compressive Strength (JCS) - MPA	11.8
Min. Normal Stress (SIGNMIN) - MPA	0.000 calculated min. value

OUTPUT

	Normal Stress (SIGN) MPA	Shear Strength (TAU) MPA	dTAU/dSIGN (DTDS)	Friction Angle (PHI) degrees	Cohesive Strength (COH) MPA
Input, or F10	0.001	0.002	1.616	58.24	0.000
	0.010	0.014	1.311	52.67	0.001
	0.050	0.062	1.141	48.76	0.005
	0.100	0.118	1.075	47.08	0.010
	0.200	0.222	1.014	45.39	0.019
	0.300	0.321	0.980	44.41	0.027
	0.400	0.418	0.956	43.71	0.036
	0.500	0.513	0.938	43.17	0.044
	0.600	0.606	0.923	42.72	0.052
	0.800	0.788	0.901	42.02	0.067
	1.000	0.966	0.884	41.48	0.082
	1.200	1.142	0.870	41.04	0.097

BARTON SHEAR FAILURE CRITERION

**ISFSI BORROW SITE - DOLOMITE FAULTS
TOFB-1 - FAULTS LOW**

INPUT FIELDS

Basic Friction Angle (PHIB) - degrees	14.0
Joint Roughness Coeff. (JRC)	2.3
Joint Compressive Strength (JCS) - MPA	4.3
Min. Normal Stress (SIGNMIN) - MPA	0.000 calculated min. value

OUTPUT

	Normal Stress (SIGN) MPA	Shear Strength (TAU) MPA	dTAU/dSIGN (DTDS)	Friction Angle (PHI) degrees	Cohesive Strength (COH) MPA
Input, or F10	0.001	0.000	0.391	21.35	0.000
	0.010	0.004	0.345	19.05	0.000
	0.050	0.017	0.314	17.44	0.001
	0.100	0.032	0.301	16.75	0.002
	0.200	0.061	0.288	16.06	0.004
	0.300	0.090	0.280	15.66	0.006
	0.400	0.118	0.275	15.37	0.008
	0.500	0.145	0.271	15.15	0.009
	0.600	0.172	0.267	14.96	0.011
	0.800	0.225	0.262	14.68	0.015
	1.000	0.277	0.258	14.45	0.019
	1.200	0.328	0.254	14.27	0.022

BARTON SHEAR FAILURE CRITERION

**ISFSI BORROW SITE - DOLOMITE FAULTS
TOFB-1 - FAULTS MEAN**

INPUT FIELDS

Basic Friction Angle (PHIB) - degrees 26.0
 Joint Roughness Coeff. (JRC) 5.5
 Joint Compressive Strength (JCS) - MPA 8.0
 Min. Normal Stress (SIGNMIN) - MPA 0.000 calculated min. value

OUTPUT

	Normal Stress (SIGN) MPA	Shear Strength (TAU) MPA	dTAU/dSIGN (DTDS)	Friction Angle (PHI) degrees	Cohesive Strength (COH) MPA
Input, or F10	0.001	0.001	0.999	44.97	0.000
	0.010	0.009	0.824	39.49	0.001
	0.050	0.039	0.717	35.65	0.003
	0.100	0.074	0.675	34.00	0.006
	0.200	0.139	0.633	32.35	0.012
	0.300	0.201	0.610	31.39	0.018
	0.400	0.261	0.594	30.70	0.024
	0.500	0.320	0.581	30.17	0.029
	0.600	0.378	0.571	29.74	0.035
	0.800	0.490	0.555	29.05	0.046
	1.000	0.600	0.543	28.52	0.057
	1.200	0.708	0.534	28.08	0.067

BARTON SHEAR FAILURE CRITERION

ISFSI BORROW SITE - DOLOMITE FAULTS TOFB-1 - FAULTS HIGH

INPUT FIELDS

Basic Friction Angle (PHIB) - degrees		38.0	
Joint Roughness Coeff. (JRC)		8.8	
Joint Compressive Strength (JCS) - MPA		11.8	
Min. Normal Stress (SIGNMIN) - MPA			0.003 calculated min. value

OUTPUT

	Normal Stress (SIGN) MPA	Shear Strength (TAU) MPA	dTAU/dSIGN (DTDS)	Friction Angle (PHI) degrees	Cohesive Strength (COH) MPA
Input, or F10	0.001	0.003	2.581	68.82	0.001
	0.010	0.021	1.770	60.53	0.004
	0.050	0.083	1.405	54.56	0.012
	0.100	0.149	1.278	51.96	0.021
	0.200	0.271	1.165	49.36	0.038
	0.300	0.384	1.104	47.84	0.053
	0.400	0.492	1.063	46.76	0.067
	0.500	0.597	1.033	45.92	0.081
	0.600	0.699	1.008	45.23	0.094
	0.800	0.897	0.971	44.15	0.120
	1.000	1.088	0.943	43.31	0.145
	1.200	1.274	0.920	42.62	0.170

BARTON SHEAR FAILURE CRITERION

**ISFSI BORROW SITE - SANDSTONE JOINTS
TOFB-2 - JOINTS LOW**

INPUT FIELDS

Basic Friction Angle (PHIB) - degrees	14
Joint Roughness Coeff. (JRC)	3.35
Joint Compressive Strength (JCS) - MPA	3.25
Min. Normal Stress (SIGNMIN) - MPA	0.000 calculated min. value

OUTPUT

	Normal Stress (SIGN) MPA	Shear Strength (TAU) MPA	dTAU/dSIGN (DTDS)	Friction Angle (PHI) degrees	Cohesive Strength (COH) MPA
Input, or F10	0.001	0.000	0.451	24.29	0.000
	0.010	0.004	0.383	20.94	0.000
	0.050	0.018	0.337	18.61	0.001
	0.100	0.035	0.317	17.60	0.003
	0.200	0.065	0.298	16.59	0.006
	0.300	0.094	0.287	16.00	0.008
	0.400	0.123	0.279	15.58	0.011
	0.500	0.150	0.273	15.26	0.014
	0.600	0.177	0.268	14.99	0.017
	0.800	0.230	0.260	14.57	0.022
	1.000	0.281	0.254	14.25	0.027
	1.200	0.332	0.249	13.98	0.033

BARTON SHEAR FAILURE CRITERION

**ISFSI BORROW SITE - SANDSTONE JOINTS
TOFB-2 - JOINTS MEAN**

INPUT FIELDS

Basic Friction Angle (PHIB) - degrees	21
Joint Roughness Coeff. (JRC)	5.99
Joint Compressive Strength (JCS) - MPA	5.5
Min. Normal Stress (SIGNMIN) - MPA	0.000 calculated min. value

OUTPUT

	Normal Stress (SIGN) MPA	Shear Strength (TAU) MPA	dTAU/dSIGN (DTDS)	Friction Angle (PHI) degrees	Cohesive Strength (COH) MPA
Input, or F10	0.001	0.001	0.860	40.69	0.000
	0.010	0.008	0.693	34.72	0.001
	0.050	0.033	0.590	30.55	0.003
	0.100	0.061	0.549	28.75	0.006
	0.200	0.114	0.508	26.95	0.012
	0.300	0.163	0.486	25.90	0.018
	0.400	0.211	0.470	25.16	0.023
	0.500	0.257	0.457	24.58	0.029
	0.600	0.303	0.447	24.10	0.034
	0.800	0.390	0.432	23.36	0.045
	1.000	0.476	0.420	22.78	0.056
	1.200	0.559	0.410	22.30	0.066

BARTON SHEAR FAILURE CRITERION (from Hoek, 2000)

**ISFSI BORROW SITE - SANDSTONE JOINTS
TOFB-2 - JOINTS HIGH**

INPUT FIELDS

Basic Friction Angle (PHIB) - degrees	32
Joint Roughness Coeff. (JRC)	8.63
Joint Compressive Strength (JCS) - MPA	7.75
Min. Normal Stress (SIGNMIN) - MPA	0.000 calculated min. value

OUTPUT

	Normal Stress (SIGN) MPA	Shear Strength (TAU) MPA	dTAU/dSIGN (DTDS)	Friction Angle (PHI) degrees	Cohesive Strength (COH) MPA
Input, or F10	0.001	0.002	1.819	61.19	0.000
	0.010	0.015	1.316	52.78	0.002
	0.050	0.062	1.066	46.83	0.008
	0.100	0.112	0.975	44.27	0.015
	0.200	0.205	0.891	41.70	0.027
	0.300	0.292	0.845	40.19	0.038
	0.400	0.374	0.813	39.12	0.049
	0.500	0.455	0.790	38.29	0.060
	0.600	0.533	0.771	37.62	0.070
	0.800	0.684	0.741	36.55	0.091
	1.000	0.829	0.719	35.72	0.110
	1.200	0.971	0.701	35.04	0.130

BARTON SHEAR FAILURE CRITERION

**ISFSI BORROW SITE - SANDSTONE BEDDING
TOFB-2 - BEDDING LOW**

INPUT FIELDS

Basic Friction Angle (PHIB) - degrees
 Joint Roughness Coeff. (JRC)
 Joint Compressive Strength (JCS) - MPA
 Min. Normal Stress (SIGNMIN) - MPA

14
5.5
3.25

0.000 calculated min. value

OUTPUT

	Normal Stress (SIGN) MPA	Shear Strength (TAU) MPA	dTAU/dSIGN (DTDS)	Friction Angle (PHI) degrees	Cohesive Strength (COH) MPA
Input, or F10	0.001	0.001	0.598	30.86	0.000
	0.010	0.005	0.474	25.37	0.001
	0.050	0.022	0.395	21.54	0.002
	0.100	0.041	0.362	19.89	0.005
	0.200	0.075	0.329	18.23	0.010
	0.300	0.107	0.311	17.27	0.014
	0.400	0.138	0.298	16.58	0.019
	0.500	0.167	0.288	16.05	0.023
	0.600	0.195	0.279	15.62	0.028
	0.800	0.250	0.267	14.93	0.037
	1.000	0.302	0.257	14.40	0.045
	1.200	0.353	0.249	13.96	0.054

BARTON SHEAR FAILURE CRITERION

**ISFSI BORROW SITE - SANDSTONE BEDDING
TOFB-2 - BEDDING MEAN**

INPUT FIELDS

Basic Friction Angle (PHIB) - degrees	21
Joint Roughness Coeff. (JRC)	6.5
Joint Compressive Strength (JCS) - MPA	5.5
Min. Normal Stress (SIGNMIN) - MPA	0.000 calculated min. value

OUTPUT

	Normal Stress (SIGN) MPA	Shear Strength (TAU) MPA	dTAU/dSIGN (DTDS)	Friction Angle (PHI) degrees	Cohesive Strength (COH) MPA
Input, or F10	0.001	0.001	0.911	42.34	0.000
	0.010	0.008	0.723	35.88	0.001
	0.050	0.034	0.609	31.35	0.004
	0.100	0.063	0.563	29.40	0.007
	0.200	0.117	0.519	27.45	0.013
	0.300	0.168	0.494	26.31	0.019
	0.400	0.216	0.477	25.50	0.025
	0.500	0.263	0.464	24.87	0.031
	0.600	0.309	0.453	24.36	0.037
	0.800	0.398	0.436	23.55	0.049
	1.000	0.484	0.423	22.92	0.061
	1.200	0.567	0.412	22.41	0.072

BARTON SHEAR FAILURE CRITERION

ISFSI BORROW SITE - SANDSTONE BEDDING TOFB-2 - BEDDING HIGH

INPUT FIELDS

Basic Friction Angle (PHIB) - degrees	32	
Joint Roughness Coeff. (JRC)	7.5	
Joint Compressive Strength (JCS) - MPA	7.75	
Min. Normal Stress (SIGNMIN) - MPA		0.000 calculated min. value

OUTPUT

	Normal Stress (SIGN) MPA	Shear Strength (TAU) MPA	dTAU/dSIGN (DTDS)	Friction Angle (PHI) degrees	Cohesive Strength (COH) MPA
Input, or F10	0.001	0.002	1.572	57.54	0.000
	0.010	0.014	1.198	50.14	0.002
	0.050	0.056	0.998	44.95	0.006
	0.100	0.104	0.923	42.71	0.012
	0.200	0.193	0.853	40.47	0.022
	0.300	0.276	0.814	39.16	0.031
	0.400	0.356	0.788	38.23	0.041
	0.500	0.434	0.767	37.51	0.050
	0.600	0.509	0.751	36.92	0.059
	0.800	0.657	0.726	35.98	0.076
	1.000	0.800	0.707	35.26	0.093
	1.200	0.940	0.692	34.67	0.110

BARTON SHEAR FAILURE CRITERION

ISFSI BORROW SITE - SANDSTONE FAULTS TOFB-2 - FAULTS LOW

INPUT FIELDS

Basic Friction Angle (PHIB) - degrees	14.0
Joint Roughness Coeff. (JRC)	1.3
Joint Compressive Strength (JCS) - MPA	3.3
Min. Normal Stress (SIGNMIN) - MPA	0.000 calculated min. value

OUTPUT

	Normal Stress (SIGN) MPA	Shear Strength (TAU) MPA	dTAU/dSIGN (DTDS)	Friction Angle (PHI) degrees	Cohesive Strength (COH) MPA
Input, or F10	0.001	0.000	0.327	18.09	0.000
	0.010	0.003	0.301	16.76	0.000
	0.050	0.015	0.284	15.83	0.001
	0.100	0.029	0.276	15.43	0.001
	0.200	0.056	0.269	15.03	0.002
	0.300	0.082	0.264	14.80	0.003
	0.400	0.109	0.261	14.63	0.004
	0.500	0.135	0.259	14.50	0.005
	0.600	0.160	0.257	14.40	0.006
	0.800	0.212	0.254	14.23	0.009
	1.000	0.262	0.251	14.10	0.011
	1.200	0.312	0.249	14.00	0.013

BARTON SHEAR FAILURE CRITERION

**ISFSI BORROW SITE - SANDSTONE FAULTS
TOFB-2 - FAULTS MEAN**

INPUT FIELDS

Basic Friction Angle (PHIB) - degrees
 Joint Roughness Coeff. (JRC)
 Joint Compressive Strength (JCS) - MPA
 Min. Normal Stress (SIGNMIN) - MPA

21
3.6
5.5

0.000 calculated min. value

OUTPUT

	Normal Stress (SIGN) MPA	Shear Strength (TAU) MPA	dTAU/dSIGN (DTDS)	Friction Angle (PHI) degrees	Cohesive Strength (COH) MPA
Input, or F10	0.001	0.001	0.646	32.87	0.000
	0.010	0.006	0.561	29.28	0.000
	0.050	0.027	0.504	26.76	0.002
	0.100	0.052	0.481	25.68	0.003
	0.200	0.098	0.458	24.60	0.007
	0.300	0.143	0.444	23.96	0.010
	0.400	0.187	0.435	23.51	0.013
	0.500	0.230	0.428	23.17	0.017
	0.600	0.273	0.422	22.88	0.020
	0.800	0.356	0.413	22.43	0.026
	1.000	0.438	0.406	22.08	0.033
	1.200	0.519	0.400	21.80	0.039

BARTON SHEAR FAILURE CRITERION

ISFSI BORROW SITE - SANDSTONE FAULTS TOFB-2 - FAULTS HIGH

INPUT FIELDS

Basic Friction Angle (PHIB) - degrees
 Joint Roughness Coeff. (JRC)
 Joint Compressive Strength (JCS) - MPA
 Min. Normal Stress (SIGNMIN) - MPA

32
5.87
7.75

0.000 calculated min. value

OUTPUT

	Normal Stress (SIGN) MPA	Shear Strength (TAU) MPA	dTAU/dSIGN (DTDS)	Friction Angle (PHI) degrees	Cohesive Strength (COH) MPA
Input, or F10	0.001	0.001	1.285	52.11	0.000
	0.010	0.011	1.046	46.28	0.001
	0.050	0.050	0.906	42.19	0.004
	0.100	0.094	0.852	40.43	0.008
	0.200	0.176	0.800	38.67	0.016
	0.300	0.254	0.771	37.64	0.023
	0.400	0.330	0.751	36.91	0.030
	0.500	0.405	0.736	36.34	0.037
	0.600	0.478	0.723	35.88	0.044
	0.800	0.620	0.704	35.15	0.057
	1.000	0.760	0.689	34.58	0.070
	1.200	0.896	0.678	34.12	0.083